EFFECT OF INITIAL SUPPORT OF EXCAVATION ON SEISMIC PERFORMANCE OF CUT AND COVER STRUCTURES

A THESIS SUBMITTED TO
THE GRADUATE SCHOOL OF NATURAL AND APPLIED SCIENCES
OF
MIDDLE EAST TECHNICAL UNIVERSITY

BY

HAMIDREZA REZAEI

IN PARTIAL FULFILMENT OF THE REQIREMENTS
FOR
THE DEGREE OF MASTER OF SCIENCE
IN
CIVIL ENGINEERING

MAY 2011

I hereby declare that all information in this document has been obtained and presented in accordance with the academic rules and ethical conduct. I also declare that, as required by these rules and conduct, I have fully cited and referenced all material and results that are not original to this work.

Name, Last Name: **HAMIDREZA REZAEI**

Signature :

ABSTRACT

EFFECT OF INITIAL SUPPORT OF EXCAVATION ON SEISMIC PERFORMANCE OF CUT AND COVER STRUCTURES

Rezaei, Hamidreza

M.Sc., Department of Civil Engineering

Supervisor: Asst. Prof. Dr. Alp Caner

MAY 2011, 66 pages

The effect of the initial support and its embedment depth, on the seismic performance of cut and cover tunnels is investigated. Cut and cover construction is one of the fastest and cheapest methods for constructing rectangular shallow tunnels. Construction of cut and cover structure in soil usually starts with installation of the initial support of excavation system, which may consists of rigid type of initial supports such as tangent piles or secant piles. These systems usually remain in place after completion of the final structure. However, to simplify the design, it is a common practice to ignore the contribution of initial support. In this study the effect of initial support of excavation on the seismic performance of cut and cover tunnels is investigated by means of a detailed dynamic finite element analysis. Three different tunnel geometries, three soil types and three acceleration histories were considered Results of the study show that depending on the soil stiffness (soft, medium, or stiff soil), the dynamic response of the tunnel deformations are affected significantly by the initial support of excavation. The effect of the initial support diminishes as the quality of the soil improves. Therefore, dynamic analyses are recommended for the final design of this type of structures especially in soft soils.

Keywords: Seismic design of cut and cover tunnels, Initial supports of the excavation, Soil-structure interaction, Simplified tunnel-ground interaction method, Free-field racking deformation of cut and cover tunnels.

Öz

ÖN KAZININ SİSTEMLERININ AÇ-KAPA TİP YAPILARDA DEPREM DAVRANIŞINA OLAN ETKİSİ

Rezaei, Hamidreza

Yüksek Lisans, İnşaat Mühendisliği Bölümü

Tez Yöneticisi: Yrd. Doç. Dr. Alp Caner

Mayıs 2011, 66 sayfa

Bu çalışma içinde ön kazı sistemleri ve ilgili gömme derinliğinin aç-kapa tünellerin deprem davranışına olan etkileri incelenmiştir. Aç-kapa tünel yapıları genellikle sığ tip olup dikdörtgen geometri yapılar kullandığı zaman hızlı yapım ve ekonomik çözümler sağlayabilmektedir. Aç-kapa tünel yapımında, genellikle ön kazı yapı sistemleri kullanmaktadır. Ön kazı yapı sistemleri rijit destekli sistemler olup tanjant kazık veya sekant kazık sistemlerinden oluşmaktadır. Bu sistemler ana yeraltı yapısı inşa edildikten sonra da yerinde kalmaktadır. Ana

yapı tasarımı sırasında ön kazı yapı sistemlerin davranışına olan etkileri mühendislik hesapları içinde yer almamaktadır. Bu çalışma içinde ön kazı yapı sistemlerinin ana yapının deprem davranışına olan etkilerini inceleyebilmek için dinamik sonlu elemanlar analizi kullanılarak inceleme yapılmıştır. Üç farklı tünel yapısı, zemin sınıfı ve deprem kuvvetli yer hareketi incelemiştir. Zemin sınıfına göre yer altı yapısının deprem etkileri altında dinamik davranışı değerlendirilmiş ve zemin sınıf iyileştikçe ön kazı yapı sistemlerinin ana yapı deprem davranışlarına olan etkisi azaldığı gözlenmiştir. Bundan dolayı zemin sınıfı zayıf olan bölgelerde bu çalışma içinde anlatılan tipten bir dinamik analiz yapmak gerekliliği ortaya çıkmıştır.

Anahtar Kelimeler: Aç-kapa yapıların sismik tasarımı, kazı için ön destek sistemleri, yapı zemin etkileşimi, basitleştirilmiş tünel ve zemin etkileşimi metodu.

To My Parents and My Family

ACKNOWLEDGEMENTS

This dissertation would not have been possible without the guidance and the help of several individuals who in one way or another contributed and extended their valuable assistance in the preparation and completion of this study.

First, my utmost gratitude to my advisor Asst. Prof. Dr. Alp Caner, whose sincerity and encouragement, patience, motivation, enthusiasm and immense knowledge I will never forget.

I would like to express my gratefulness to DR. Alper Uçak for his invaluable contributions while reviewing the draft of this thesis. I would also like to thank him due to his kind and patient personality.

I would like to thank Prof. Dr. Çetin Yilmaz, Prof. Dr. Ufuk Ergun, Assoc. Prof. Dr. Ahmet Türer, and Mehran Rezazadeh for their encouragement, insightful comments, and hard questions

I would like to express my special thanks to Dr. Joe Wang for sharing his deep knowledge with me and for his support.

Last but not the least; I would like to offer my most sincere thankfulness to my family since they have always been by my side throughout my life. I would like to express my deepest gratefulness, to my dear wife, Melody for her continuous support, endless understanding during the thesis period.

TABLE OF CONTENTS

LIST OF TABLES

TABLES

LIST OF FIGURES

FIGURES

CHAPTER 1

INTRODUCTION

1.1 Introduction

Underground facilities and infrastructures are part of every developed society all around the word. Today, living in a metropolitan area without constructing and utilizing underground facilities is almost impossible. The use of underground facilities and infrastructures is the result of lack of space for those facilities aboveground and the requirement of having that infrastructure below grade. Using underground space makes it possible to build facilities that are necessary for the community and are not suitable to be built above ground, or will not be functional if they are constructed otherwise. Transportation hubs, metro stations, and substation facilities are some examples for these types of the structures. Underground construction allows us to build in the proximity of the existing facilities and in highly populated urban areas without destroying the static and functionality of the surroundings.

Cut and cover construction is one of the methods used to build underground facilities. It is one of the fastest and cheapest methods for constructing rectangular tunnels and facilities especially if the structure is not very deep. This method is mostly preferred when the cross section of the structure is rectangular and access from the surface is possible. Construction of cut and cover structure usually starts with installation of the initial support of excavation system, which may consists of slurry walls, tangent piles, or secant piles. Then a trench between these initial supports is excavated. The structure is constructed (final liner) in the trench, and finally covered with soil. The initial support system usually remains in the place after completion of the final structure. Removal of the initial support of excavation in most cases is impossible or uneconomical. Therefore, unless it is required by the design, and future functionality of the structure, it is a common practice to leave the initial support of excavation in place after construction is completed.

Seismic behavior of the underground structures is a complicated phenomenon. For a long time it was believed that, the seismic design for underground structures was not necessary. Based on the performance record, it is fair to say that underground structures are less vulnerable to earthquakes than surface structures (Dowding and Rozen 1978, Rowe 1992).

On the other hand, significant damages to the underground facilities due to earthquakes have also been reported. After the 1971 San Fernando earthquake, ASCE (1974) published the damage in Los Angeles area to underground structures. Stevens (1977), Wang (1985), Sharma and Judd (1991), Power et al. (1998), and Kaneshiro et al. (2000), also have reported significant damage to the tunnels and underground facilities during various earthquakes.

One common conclusion among all these studies is that underground structures cannot be assumed safe if they are not designed and constructed properly to resist seismic forces. Another important outcome was that underground facilities constructed in the soil are more susceptible to damage due to earthquake, compared to the ones constructed in the rock.

While seismic analyses and design guidelines have been well established for bridges, and above ground structures, seismic design of underground facilities has received very little attention in the past (Wang 1993). Usually, simplified procedures based on the relative stiffness between the soil and the cut and cover structure are used in the design. For most of the engineers, it is a common practice to ignore the existence and contribution of initial support of excavation system for both static and seismic design. This may be an acceptable and conservative practice for service load design. Nevertheless, the effect of the initial support of excavation system on the dynamic properties and the dynamic response of a cut and cover structure is not well known, and not easy to predict.

1.2 Objectives

The purpose of this study is to investigate the effect of the initial support of excavation, and its embedment depth, on the seismic performance of cut and cover structures. Using the finite element technique, the effect of the initial support of excavation system on the response characteristics of cut and cover structures will be investigated. This will be done by comparing the seismic demand of the box shaped tunnels, both with and without the initial support of excavation system.

1.3 Organization

The organization of this thesis is as follows:

In Chapter 2 some basics about cut and cover structures will be presented. Different types of the initial support of excavation systems and their construction methods will be briefly presented. Design loads and procedures for the cut and cover structures will be briefly explained as well.

Chapter 3 will review the seismic analyses and design producers for cut and cover structures.

In Chapter 4, modeling assumptions and procedures used in this study will be explained in detail. The tunnel geometries, properties of the soil, initial support of the excavation, and the final liner will be given. The ground motion time histories used in the dynamic analyses and their response spectra will be presented as well.

In Chapter 5 the analyses results are presented in detail.

Finally, Chapter 6 will present the conclusions and recommendations.

CHAPTER 2

CUT AND COVER STRUCTURES

2.1 Introduction

Cut and cover is a simple method of construction that is generally used for shallow tunnels, subway stations, and some underground facilities. This method is preferred if the underground facility or tunnel is near the grade and the geometry is rectangular. Construction usually starts with excavation of a trench slightly larger than the final structure. Then the structure is constructed (final liner) in the trench, and finally covered with soil. Figure 2-1 shows a typical construction site of cut and cover tunnel.

Figure: 2-1 Cut and cover Tunnels (C. Jeremy Hung et al 2009)

There are two basic construction techniques for constructing cut and cover structures:

- Bottom-up method
- Top-down method

In the bottom-up method, after providing the initial support of excavation system, a trench is fully excavated and the tunnel is constructed by casting the invert (floor slab), walls, and finally the tunnel roof. The tunnel may be of cast in place concrete, precast concrete, or steel bents filled with concrete infill between each bent. The trench is then backfilled compacted, and the surface is prepared according to its final use. Figure 2-2 shows the construction sequence of a cut and cover tunnel using bottom-up method.

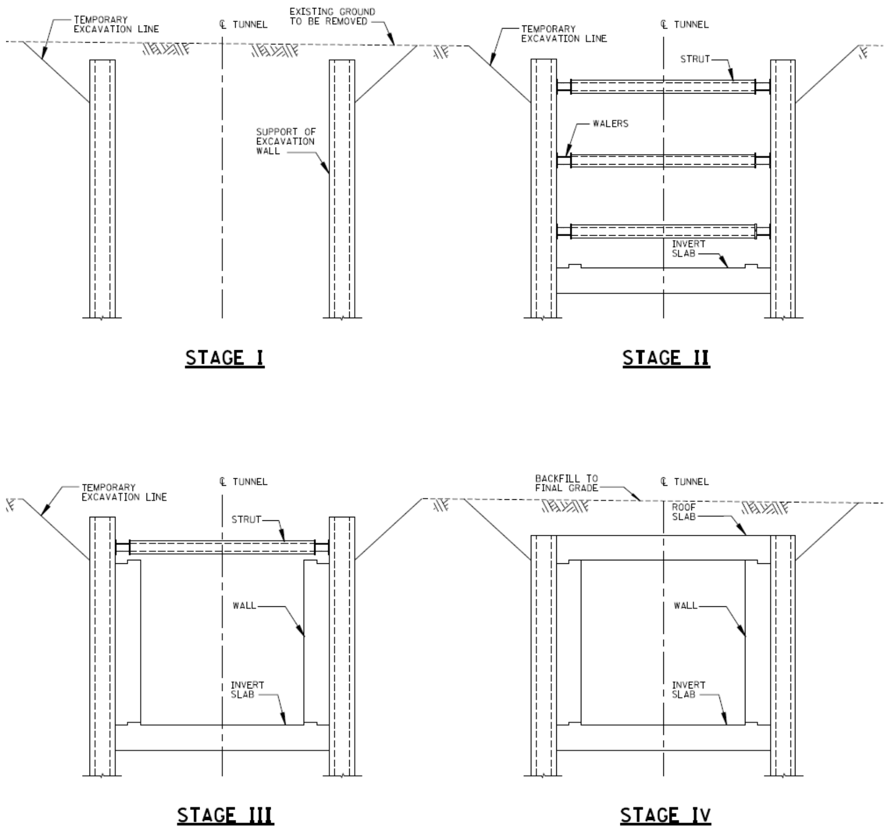

Figure 2-2: Bottom-up method construction sequence

In the top-down method, side support walls and capping beams are constructed from ground level, using slurry wall, bored piles, or secant piles. A shallow excavation is made to allow the tunnel roof to be constructed using precast beams or cast in place concrete. The surface work is then completed to serve its final function. This allows early restoration of roadways, and services. Excavation machinery is lowered into the excavation area, and the main excavation is carried out under the permanent tunnel roof, followed by constructing the base slab and internal walls as planned. Figure 2-3 shows this method schematically.

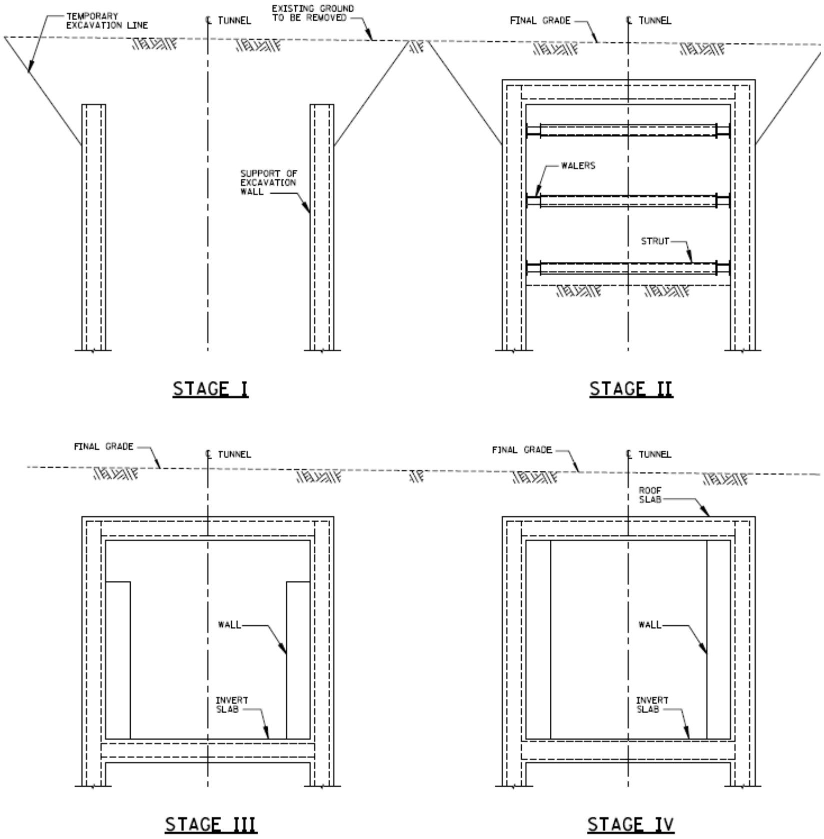

Figure 2-3: Top-down method construction sequence

2.2 Initial Support of Excavation

The support of excavation systems as defined in the Technical Manual for Design and Construction of Road Tunnels (C. Jeremy Hung et al 2009) are:

- Open cut slope: This method is used in areas where sufficient room is available to excavate a wide area, then the final structure will be constructed in segments and open cut area will be backfilled to the required elevation
- Temporary: This is a structure designed to support the excavation area as a vertical wall against soil lateral pressure and protects adjacent structures' foundation against any movement. It will either be left in place or will be removed after construction is complete. Sheet pile walls and soldier pile and laggings are mostly used for this type of support system.
- Permanent: This structure is designed and constructed to support vertical faces of the excavation. Initial support of the excavation walls will be part of the permanent tunnel structure. Slurry walls, secant pile walls, or tangent pile walls are mostly used as permanent support system.

Furthermore, the initial support of excavation systems can be classified as flexible and rigid.

2.2.1 Flexible Support

Flexible supports of excavation examples are sheet piling, and soldier pile and lagging walls. These types of supports have many limitations in application and are not suitable for relatively deep excavation or construction in areas that are close to structures that cannot tolerate large settlements or deflections. They are also not rigid and durable enough to be part of load resisting system for final structure. Therefore, in practice these types of support are mostly ignored in the final design of structures.

2.2.2 Rigid Support

Rigid supports of excavation, such as slurry walls, secant piles, or tangent piles are very stiff, and they could be used as final structure for resisting lateral loads. In most cases, construction of an initial support system to protect structures that are in the vicinity of the excavation and to minimize the obstruction in the excavation area requires a rigid type of initial support system.

Next section will explain different types of rigid initial support system and their construction methods in detail.

2.2.2.1 Slurry Wall

Slurry wall is constructed by excavating a trench usually 80 cm to 150 cm thick, as it is required by the design. As excavation of the trench is progressing, it is stabilized by placement of bentonite slurry in place of the soil that is excavated. This excavation has to be extended as deep as it is required by the design for stability of the wall or if the bedrock elevation is high enough it will penetrate into it, until it can be assumed fixed at the bottom. Reinforcement steel or in most cases wide flange steel beams will be placed in the trench and the slurry is replaced by placing concrete from bottom to the top of the trench and removing the bentonite slurry as concrete is added. During the excavation, additional bracing such as struts or tiebacks will be used as required.

2.2.2.2 Tangent Pile Wall

Tangent pile walls are constructed by drilling circular shafts next (tangent) to each other along the excavation area. These shafts are 60 cm to 120 cm in diameter. Like slurry wall system, these piles have to extend below the invert level or lock into the rock, if it is possible. Steel casing will be used to keep the drilled shaft area open, during the soil removal. After drilling is complete, steel beams or reinforcement bars are placed in, and the shaft is filled with concrete. Steel casing can be removed as the concrete is placed in the shaft. Again, during the excavation additional support might be required for stability of the wall. Figure 2-4 is shows the construction sequence of a tangent pile system.

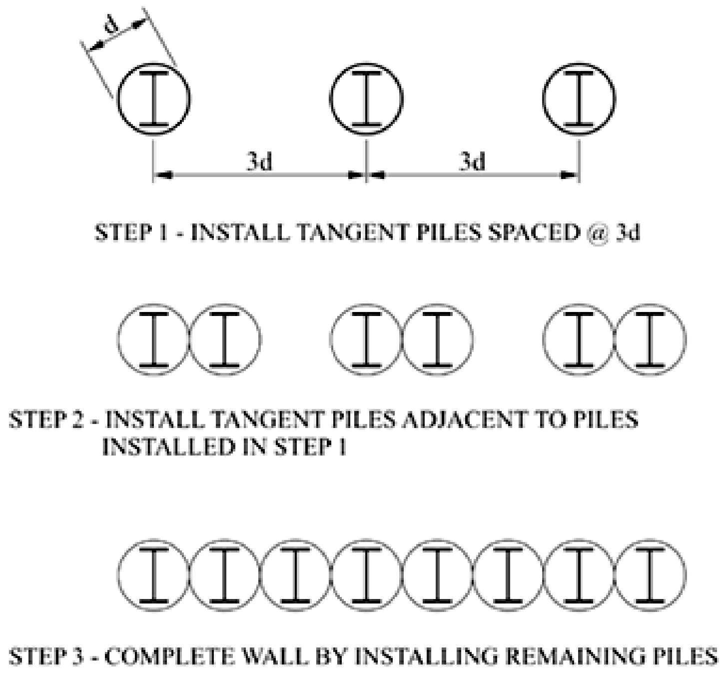

Figure 2-4: Tangent pile wall construction sequence (C. Jeremy Hung et al 2009)

2.2.2.3 Secant Pile Wall

Secant pile walls are constructed in a similar way that tangent pile walls are constructed. The only difference is that the drilled shafts have some overlap. This provides some more stiffness and water tightness for areas with high ground water elevation. Figure 2-5 shows a completed secant pile wall.

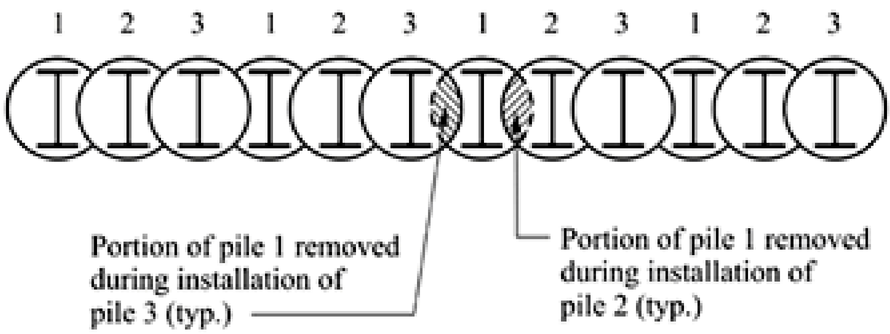

Figure 2- 5: Completed secant pile wall (C. Jeremy Hung et al 2009)

2.3 Design Procedure for Cut and Cover Structures

All components of cut and cover structures shall be designed to sustain the most severe combination of service loads, such as, dead and live loads, surcharge, hydrostatic, earth pressure, shrinkage, thermal, differential settlement, impact loads due to train derailment, and seismic loads to which they may be expected to be subjected at any time. Based on an assumed construction sequence the effect of erection and other temporary loads occurring during construction shall be considered as well.

All design loads shall be combined according to applicable codes and specifications. Symmetrical and asymmetrical loadings are two major loading types that will create primary load combination for cut and cover structures.

Figures 2-6 and 2-7 depict schematic presentation of the loads acting on a typical cut and cover tunnel for top-down and bottom-up construction in soil respectively.

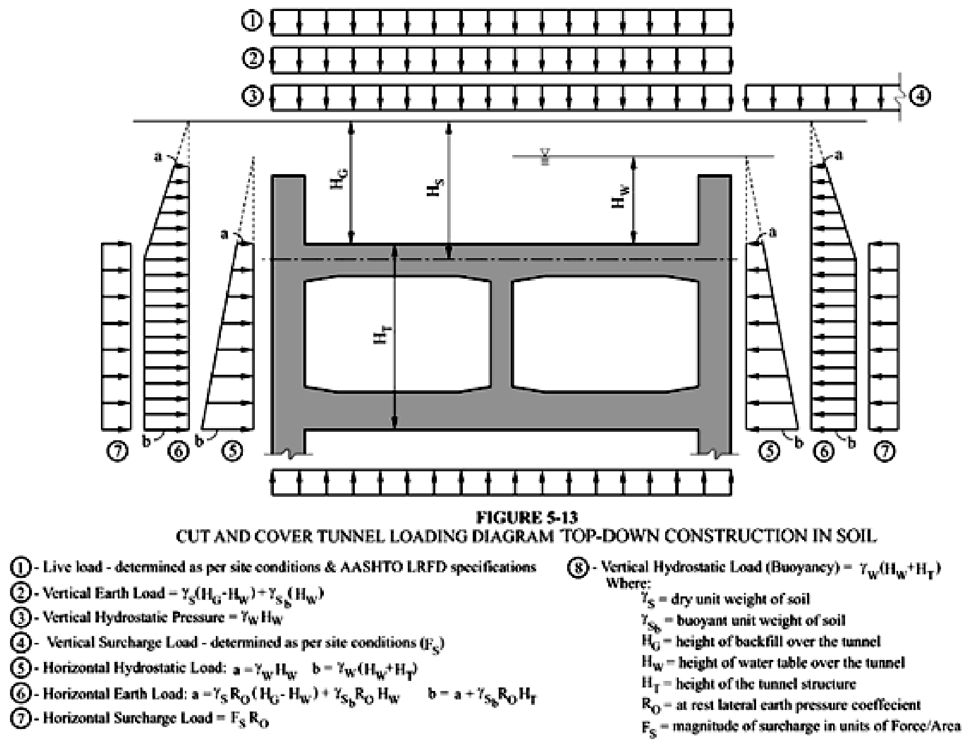

Figure 2- 6: Typical loads acting on cut and cover tunnel Top - down construction (C. Jeremy Hung et al 2009)

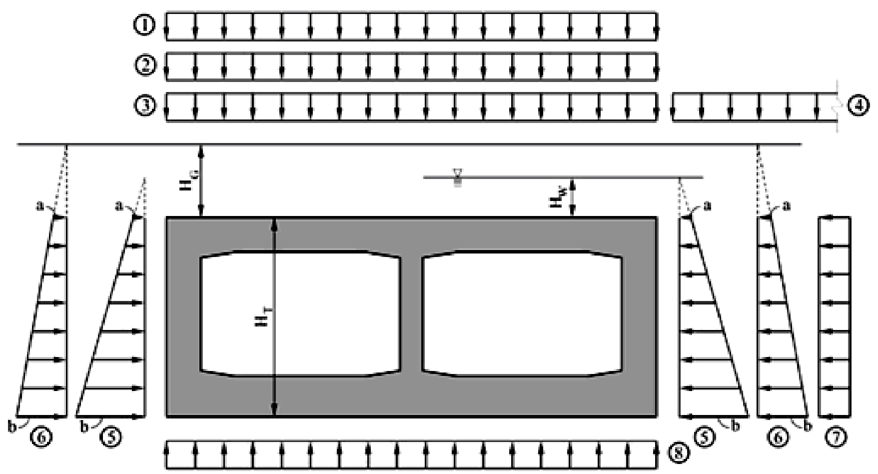

FIGURE 5-12
CUT AND COVER TUNNEL LOADING DIAGRAM - BOTTOM UP CONSTRUCTION IN SOIL

① - Live load - determined as per site conditions & AASHTO LRFD specifications
② - Vertical Earth Load = $\gamma_S(H_G - H_W) + \gamma_{S_b}(H_W)$
③ - Vertical Hydrostatic Pressure = $\gamma_W H_W$
④ - Vertical Surcharge Load - determined as per site conditions (F_S)
⑤ - Horizontal Hydrostatic Load: $a = \gamma_W H_W$ $b = \gamma_W (H_W + H_T)$
⑥ - Horizontal Earth Load: $a = \gamma_S R_O (H_G - H_W) + \gamma_{S_b} R_O H_W$ $b = a + \gamma_{S_b} R_O H_T$
⑦ - Horizontal Surcharge Load = $F_S R_O$
⑧ - Vertical Hydrostatic Load (Buoyancy) = $\gamma_W (H_W + H_T)$

Where:
γ_S = dry unit weight of soil
γ_{S_b} = buoyant unit weight of soil
H_G = height of backfill over the tunnel
H_W = height of water table over the tunnel
H_T = height of the tunnel structure
R_O = at rest lateral earth pressure coeffecient
F_S = magnitude of surcharge in units of Force/Area

Figure 2- 7: Typical loads acting on cut and cover tunnel Bottom- up construction (C. Jeremy Hung et al 2009)

CHAPTER 3

REVIEW OF SEISMIC DESIGN PROCEDURES FOR CUT AND COVER STRUCTURES

3.1 Introduction

Underground facilities, such as tunnels, are a crucial part of the transportation infrastructure. Due to their strategic importance, loss of functionality in an earthquake is not an acceptable performance criterion for tunnels. It is expected that tunnels can withstand the maximum credible earthquake without significant damage and loss of their function. While the structural performance of underground facilities during the past earthquakes were considerably better than the performance of bridges or above ground facilities (Dowding and Rozen 1978; Rowe 1992), significant structural damage has been reported during the 1971 San Fernando and 1995 Kobe earthquakes (C. Jeremy Hung et al 2009), see also Figure 3-1.

Figure 3-1: Reinforced concrete column failure observed in a cut-and-cover tunnel during 1995 Kobe Earthquake (C. Jeremy Hung et al 2009)

Seismic analyses and design procedures and guidelines are well established for bridges, and above ground structures. However, seismic design of underground facilities has received very little attention in the past. In fact, prior to 1960's, earthquake loading was not accounted for in the design process of underground structures (Wang 1993). Even today, there are very few, or no seismic design provisions for tunnels in most design codes.

3.2 Review of Seismic Analysis Procedures for Rectangular Tunnels

Analytical studies conducted in the last thirty years show that cut and cover tunnels are subjected to racking, axial and curvature deformations during a seismic event (Owen and Scholl 1981, Wang 1993). Figure 3-2 and 3-3 illustrate these three deformation modes schematically.

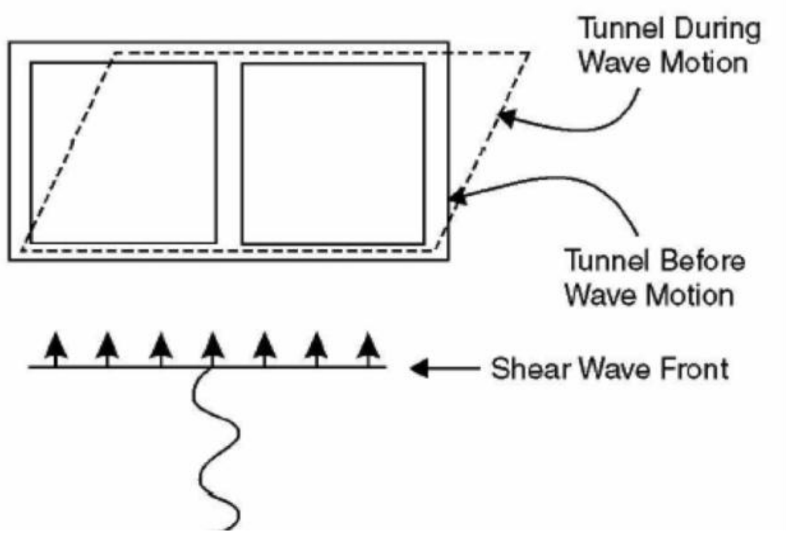

Figure 3-2: Racking deformation of a rectangular tunnel under vertically propagating shear waves (Wang 1993)

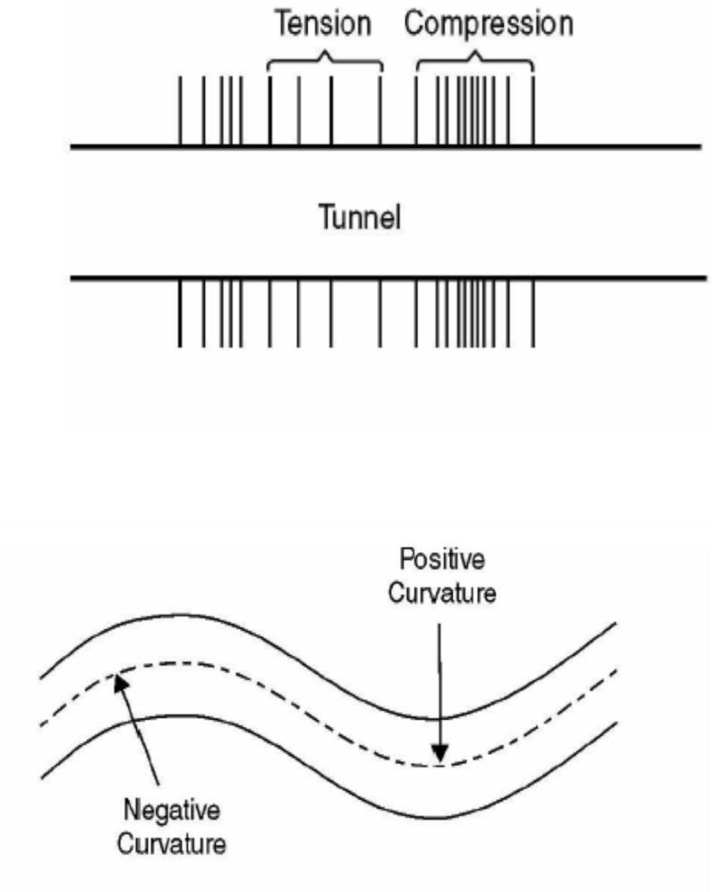

Figure 3-3: Axial and curvature deformation of tunnels under seismic loading (Owen and Scholl 1981)

As discussed in detail by Owen and Scholl (1981) and Wang (1993), the racking deformation caused by the vertically propagating shear waves is considered the most critical response of a rectangular cut and cover structure. Hence, different methods are proposed to determine the racking deformation of cut and cover structures.

These methods are categorized into three groups, namely:

- pseudo-static method
- free-field racking deformation method
- simplified tunnel-ground interaction method

These methods are explained in more details next.

3.2.1 Pseudo-static Methods

Pseudo-static methods, such as the Mononobe-Okabe method (Okabe 1926, Mononobe and Matsu 1929) or the procedure proposed by Wood (1973) are used to determine the dynamic earth pressure acting on the side walls of underground cut and cover structures (Anderson et al. 2008). The pseudo-static methods are usually based on the peak ground acceleration of the maximum creditable earthquake, and they ignore the frequency content of the ground motion.

The Mononobe-Okabe method, which was originally developed for seismic analysis of above ground yielding retaining walls, inherently assumes that the (above ground) retaining wall can tilt and/or move such that a Coulomb type soil wedge can form in the back-fill. Thus, the pseudo-static active earth pressure caused by the dynamic excitation is assumed to be due to the inertia force acting on the wedge. However, as discussed by Wang (1993), Hashash et al. (2001), and Hung et al. (2009), this assumption, that is, the tilting and/or moving wall, is not applicable for underground structures. During a seismic event, the cut and cover structure and the surrounding soil will move together, and a Coulomb type soil sliding wedge, will not form. Consequently, the “Mononobe-Okabe” method will provide unrealistic results. The data and subsequent detailed analysis done by Ostadan (1997) have clearly shown that the seismic soil pressure is a result of the interaction between the soil and the structure during a seismic event. In fact, the deeper the tunnel embedment, the less realistic become calculated forces using the “Mononobe-Okabe” method. In fact, the effect of the structure's embedment and variation of the seismic forces with depth is not measurable in this method.

On the other hand, the analytical solution proposed by Wood (1973) is valid for non-yielding rigid buried walls. Although, the solution is based on dynamic modal analysis, in practice a horizontal pseudo-static body force is applied to the buried non-yielding rigid wall. Cut and cover tunnels are relatively flexible structures, and due to the rigid wall assumption, Wood method is not recommended for seismic design of such structures. In addition, this method does not include the wave propagation and amplification of the motion due to the geometry of the structure and soil properties.

3.2.2 Free-Field Racking Deformation Method

In the free-field racking deformation method, the stiffness of the underground structure is ignored, and the displacement demand of the underground structure subjected to a seismic event (that is racking demand) is assumed to be equal to the free-field deformation. Schematic presentation of this popular procedure, which is used in the design of San Francisco BART subway stations (Kuesel 1969) and Los Angles Metro project (Merritt 1991), is given in Figure 3-4.

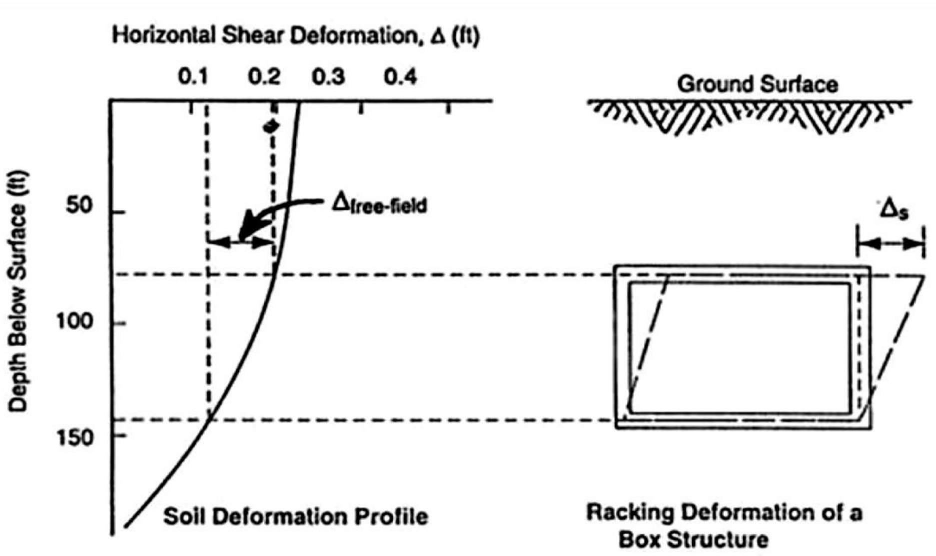

Figure 3-4: Schematic presentation of the free-field racking method (Wang 1993)

While the free-field racking deformation method is very attractive due to its simplicity, it will produce realistic results only if the flexibility of the underground structure is comparable with the surrounding soil medium. However, the stiffness of a cut and cover tunnel located in soft soil can be much higher than the stiffness of the soil, such that it may deform less than the medium. In such cases, the free-field racking deformation method will produce very conservative demand estimates, as demonstrated by Wang (1993). This method is suitable for cases that the ground distortions are small.

3.2.3 Simplified Tunnel-Ground Interaction Analysis

Performing dynamic analysis on berried structures and tunnel are much more complicated compared to the above ground structures. Closed form solutions for tunnel-ground interaction are available for circular tunnels but due to the variable geometric characteristics of the cut and cover rectangular tunnels, these types of solutions are not available for cut and cover structures. Therefore, a simplified tunnel-ground interaction method will be a useful tool for engineers to overcome this problem.

Wang (1993), Penzien (2000), Nishioka and Unjoh (2003) proposed simplified tunnel-ground interaction curves to be used in the seismic analysis and design of cut and cover structures.

Wang (1993) conducted a series of finite element studies to study the dynamic response of cut and cover structures. In the finite element analyses, the soil medium and the structure are assumed to be (equivalent) linear elastic and no-slip between soil and concrete is assumed (Wang 1993). Based on the analyses, Wang (1993) reported that the seismic demand of a cut and cover structure was influenced by the relative stiffness of the underground structure with respect to the surrounding soil, structure geometry and embedment depth of the tunnel, in addition to the characteristics of the ground motion corresponding to the design earthquake.

Based on thirty-six dynamic finite element analyses, Wang (1993) concluded that the seismic racking demands in a cut and cover structure could be expressed as a function of flexibility ratio F_r, defined as (Wang 1993):

$$F_r = \frac{G_m W}{K_s H} \tag{3-1}$$

in equation (3-1):

G_m : the average (equivalent or strain-compatible) shear modulus of the soil

K_s : the racking stiffness of the cut and cover structure

W : the width of the cut and cover structure

H : the height of the cut and cover structure

Based on the flexibility ratio calculated using equation (3-1), the racking coefficient is given as (Wang 1993):

$$R_r = \frac{\Delta_s}{\Delta_{ff}} = \frac{4(1-\nu_m)}{3-4\nu_m+F_r} \tag{3-2}$$

in equation (3-2):

υ_m : the Poisson's ratio of the medium

Slip between the cut and cover tunnel and the soil medium were investigated later by Penzien (2000). Based on a series of finite element analyses, Penzien (2000) proposed a racking coefficient, which reads:

$$R_r = \frac{\Delta_s}{\Delta_{ff}} = \frac{4(1-\nu_m)F_r}{2.5-3\nu_m + F_r} \tag{3-3}$$

Figure 3-5 compares the racking coefficient functions proposed by Wang (1993), and Penzien (2000). From Figure 3-5, it can be observed that the contribution of slip on the raking response is negligible. Furthermore, Figure 3-5 shows that when the flexibility ratio is equal to unity, the racking coefficient is also equal to unity. In other words, when the soil stiffness equals to the structure stiffness, the racking deformation equals to the free-field deformation. When the flexibility ratio is less then unity, the free-field deformation is de-amplified, that is, the racking deformation is less than the free-field deformation. When the flexibility ration is above unity (stiff soil, flexible tunnel) ground motion will amplify, such that the racking deformation is larger than the free-field deformation.

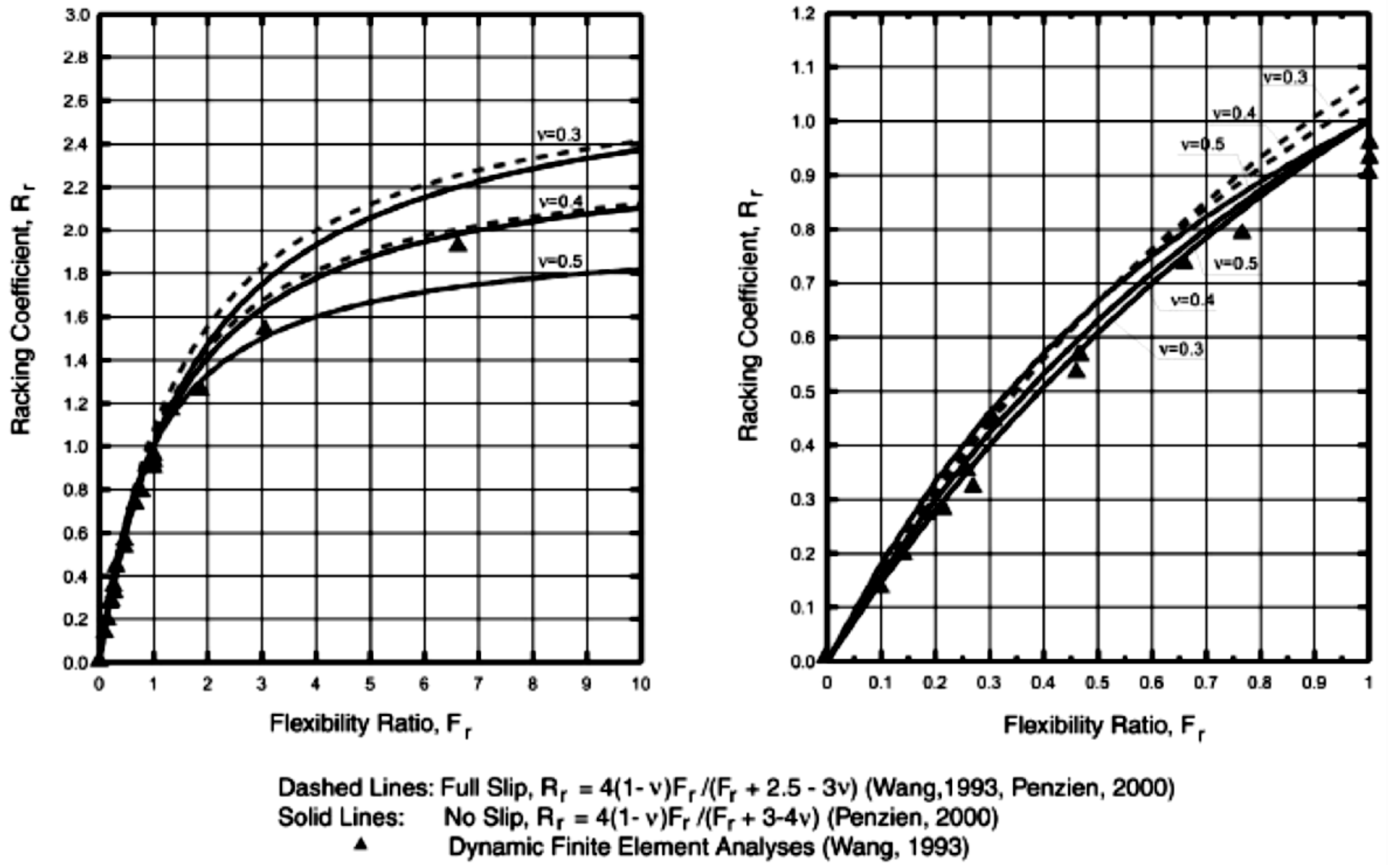

Figure 3-5: Racking coefficient for rectangular tunnels (C. Jeremy Hung et al 2009)

CHAPTER 4

FINITE ELEMENT MODELING ASSUMPTIONS AND PROPERTIES

4.1 Tunnel Geometry

This chapter is devoted to the discussion of finite element models used in this study. To investigate the effect of the support of excavation and its embedment depth on the seismic behavior of cut and cover tunnels, three different geometries are selected. Case A, consist of a 10 m by 10 m square concrete box. Case B is a 10 m height by 20 m wide rectangle, with a 1.2 m column at the center of the tunnel. Finally, case C is a duplicate of case B, with exception of the center column. Liner thickness is assumed to be 1.2 m thick concrete section for all cases. Gross section properties are used for all members in analyses. For all cases the over burden is assumed to be 10 m, and the bedrock is assumed to be 80 m below grade level. Figure 4-1 shows the schematic presentation of the tunnel geometries used in the study.

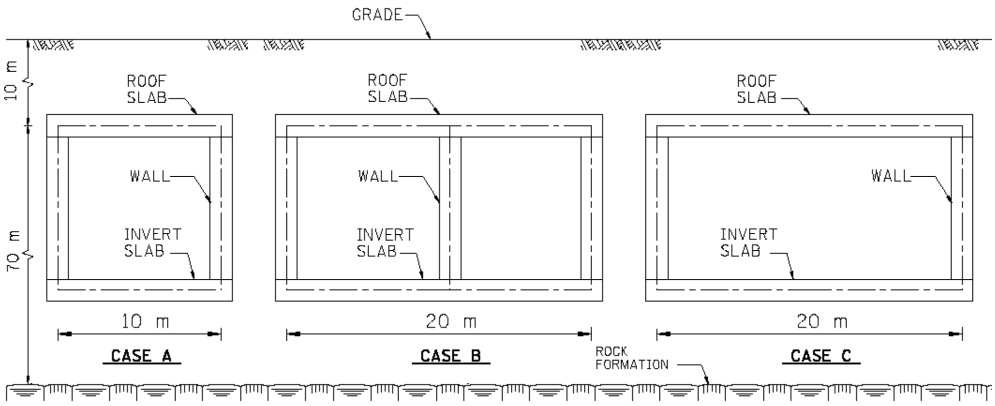

Figure 4-1: Schematic presentation of the tunnel geometries used in the study

4.2 Support of Excavation System

Stiffness and strength requirements of the initial support systems depend on the different parameters. Soil condition, existing and construction surcharges, and their distance to the excavation area, excavation depth, ground water table elevation, and type of support system are some of the important parameters for selection of the initial support of the excavation. To simplify the parametric study, support of excavation is assumed 1.2 m thick concrete section for all the cases. To study the effect of the embedment length of the initial support (denoted with “L” in Figure 4-2), three different embedment lengths, are assumed, namely 2.5 m, 5 m, and 7.5 m. The schematic presentations of the tunnel geometries with the initial supports are depicted in Figures 4-2, 4-3, and 4-4.

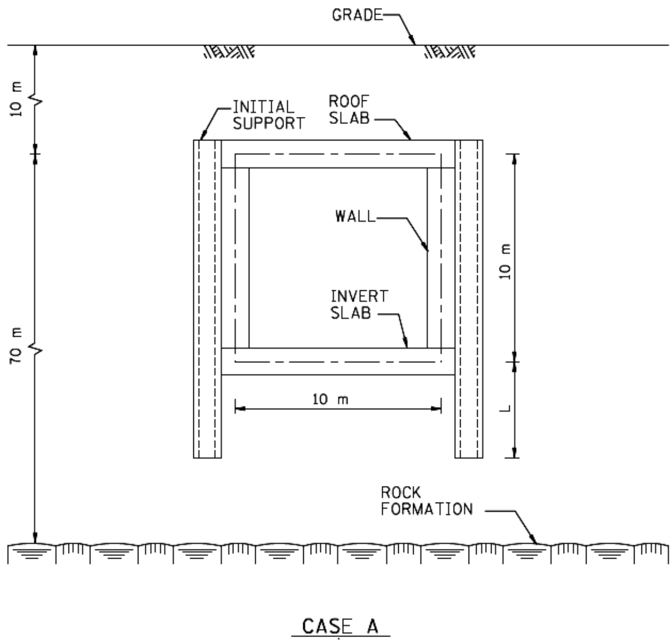

Figure 4-2: Case A with initial support

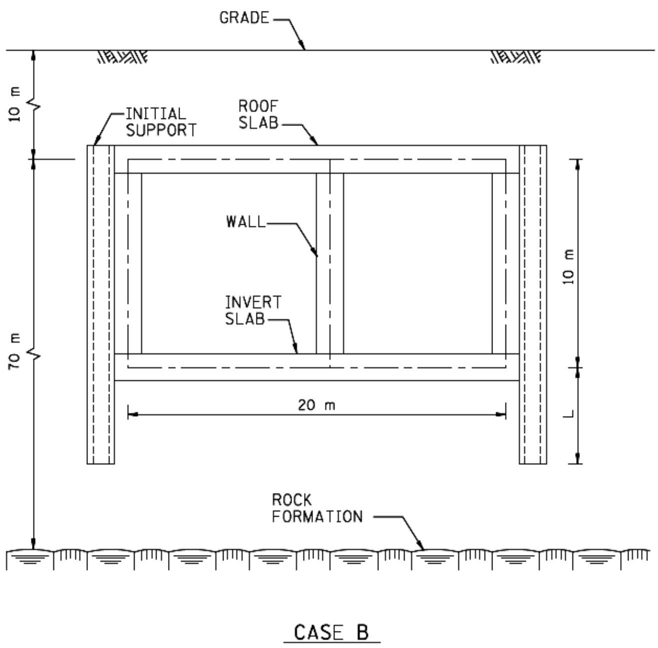

Figure 4-3: Case B with initial support

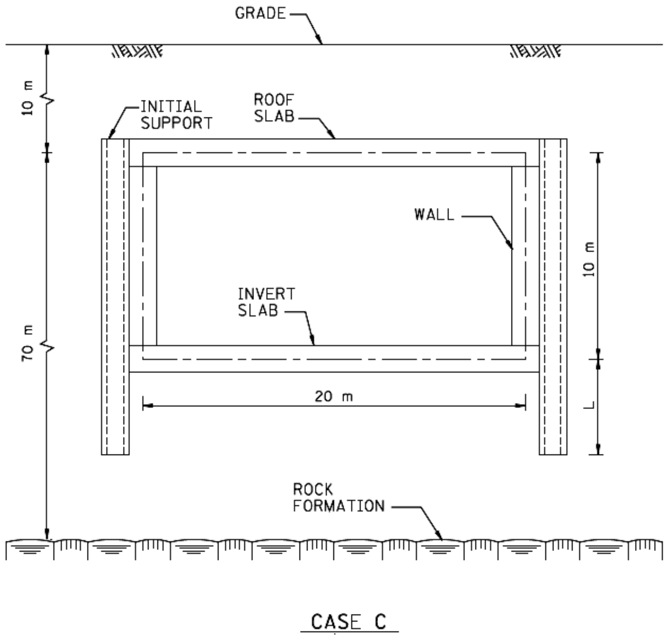

Figure 4-4: Case C with initial support

4.3 Soil Properties

To study soil effects, three different soil types are considered for this study. The unit weight of the soil assumed to be equal (17 KN/m^3) for all cases. One of the most important soil parameters for seismic design is the shear wave velocity of the soil. In the current design codes site classifications are based on the mean shear wave velocity of the upper 100 ft. (~30 m) of the soil profile. In this study, three different mean shear wave velocities, 100 m/s, 200 m/s, and 400 m/s selected and referred as soil type I, soil type II, and soil type III respectively. These values are representing site class E, D, and C in the International Building Code, AASHTO, and ASCE 7. Site class C represents, very dense soil and soft rock with shear wave velocity from 370 m/s to 760 m/s. Site class D represents, stiff soil profile with mean shear wave velocity between 180 m/s to 370 m/s. Site class E, is usually, a weak soil profile with shear wave velocity less than 180 m/s. Table 4-1 shows properties of the three types of soils used in the finite element analyses. In Table 4-1, ν is the Poisson's ratio; γ is the soil unit weight; V_s is the mean shear wave velocity; E and G are the modulus of elasticity and shear modulus respectively. In this study, the unit weight, and mean shear wave velocity, for each soil type are entered as the input for soil properties and E and G values are calculated in PLAXIS (version 8) accordingly.

Table 4-1: Soil parameters for FE study

Parameter	**Soil Type I**	**Soil Type II**	**Soil Type III**
ν(-)	0.462	0.30	0.30
γ (KN/m^3)	17	17	17
Vs (m/s)	100	200	400
E (KN/m^2)	50710	180000	722000
G (KN/m^2)	17400	69400	278000

4.4 Tunnel Liner and Initial Support of Excavation Properties

Table 4-2 shows structural properties (for one-meter length) of the liner and initial support. Both liner and initial support are assumed 1.2 m thick concrete sections. Walls, invert, and roof thicknesses are selected based on some actual cases that are designed by the author with some minor modifications for simplicity. As a rule of thumb, the thickness of the members, for preliminary design, can be assumed as one eight to one tenth of the clear span of each member. In this study, all parameters are calculated based on gross section properties of the members. Full shear transfer is assumed between liner and initial support of the excavation system due to irregularity or high roughness between these two surfaces. In Table 4-2; A is the cross sectional area; I is the moment of the inertia; W is the unit weight of the members, and E is the modulus of the elasticity for the concrete.

Table 4-2: Tunnel liner and initial support properties

Parameter	Liner/Initial Support Only	Liner + Initial Support
Thickness(m)	1.20	2.40
EA (KN/m)	29785000	59571000
EI (KNm^2/m)	3574200	28594000
W (KN/m/m)	8.30	16.60

4.5 Strong Ground Motion Data

Strong motion records obtained from Pacific Earthquake Engineering Research Center’s (Peer) are used in the dynamic finite element analyses. Table 4-3 shows the earthquake and station details, peak ground acceleration (PGA), peak ground velocity (PGV), and peak ground displacement (PGV) for the used acceleration time histories. Figure 4-5 shows the acceleration time history for each motion. Figure 4-6 shows the 5% damped response spectrum for these time histories.

Table 4-3: Properties of Strong Ground Motion records

Earthquake	Duzce	C. Mendocino	Loma Prieta
Station	Bolu	Petrolia	Gilroy
Date	1999/11/21	1192/01/25	1989/10/18
Record	DUZCE	CAPEMEND	LOMAP
Component	BOL090	PET000	G01000
PGA (g)	0.822	0.590	0.411
PGV (cm/s)	62.1	48.4	31.6
PGD (cm)	13.55	21.74	6.38
PGA/PGV	0.0132	0.0122	0.0130

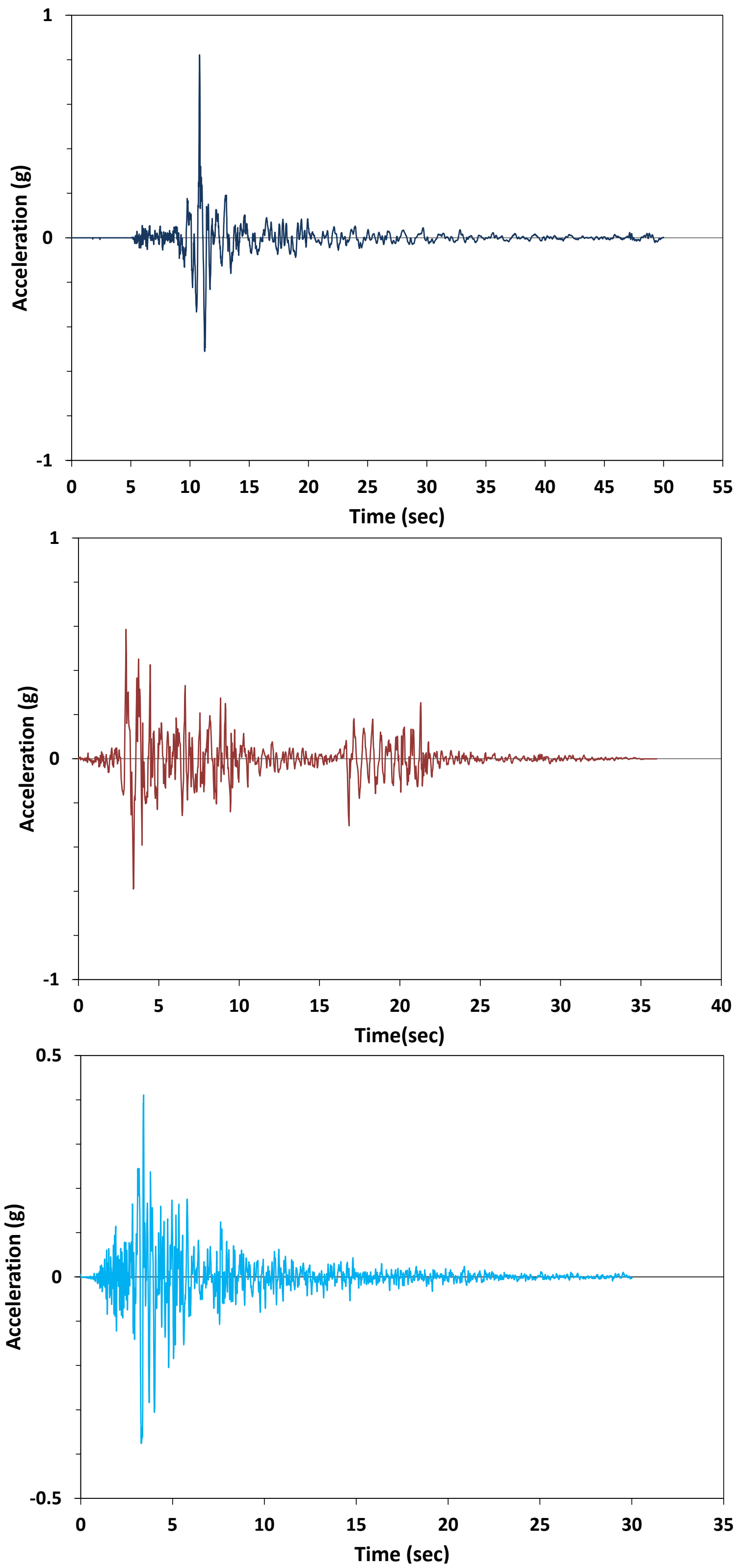

Figure 4-5: Ground motion time histories

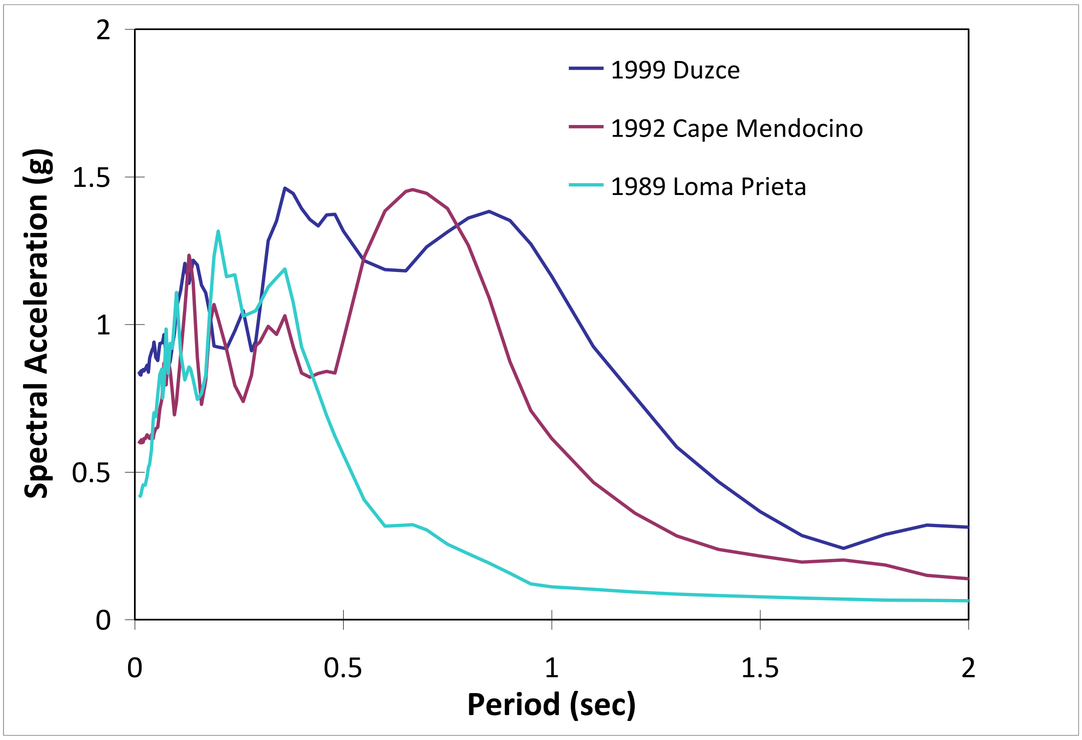

Figure 4-6: 5% Damped response spectrum of the time history records

4.6 Material Damping

Rayleigh damping is assumed in the finite element analyses. Rayleigh damping is proportional to the mass and stiffness of the system and can be expressed as:

$$C = \alpha M + \beta K \qquad (4\text{-}1)$$

Where, C represents the damping, M is the mass, and K represents the stiffness of the system. The damping ratio for the nth mode of such a system is:

$$\zeta_n = \alpha \frac{1}{2\omega_n} + \beta \frac{\omega_n}{2} \tag{4-2}$$

The Rayleigh damping coefficients, α and β should be determined from at least two different given damping ratios ζ_i and ζ_j for two frequencies of vibrations ω_i and ω_j using the following equation (PLAXIS Manual Version 8.0):

$$\alpha + \beta\omega_i^2 = 2\omega_i\zeta_i \tag{4-3}$$

This equation shows that if two damping ratios at given frequencies are known, α and β can be calculated by solving two equations simultaneously.

On the other hand, based on experimental data, it is reasonable to assume that both modes have same damping ratio ζ, and determining α and β using the following equations (Chopra):

$$\alpha = \zeta \frac{2\omega_i\omega_j}{\omega_i + \omega_j} \tag{4-4}$$

$$\beta = \zeta \frac{2}{\omega_i + \omega_j} \tag{4-5}$$

In this study, the damping ratio is assumed to be 5% and for all modes.

The frequencies for each mode are calculated using equations (4-6) and (4-7):

$$f_n = (2n-1)\frac{v_s}{4H} \tag{4-6}$$

$$\omega_n = 2\pi \times f_n \quad \ldots \tag{4-7}$$

Where,

f: The cyclic frequency

ω: The circular frequency

n: number of the mode to be calculated

v_s: Mean shear wave velocity for soil type, and

H: The height of the soil above the base rock

To calculate Rayleigh damping coefficients, the (cyclic) frequencies for the first and fifth mode of each soil type are calculated using Equation 4-6. These values are converted to the circular frequency using Equation (4-7). Assuming 5% damping for both modes and using calculated frequencies, Rayleigh damping coefficients α and β, are calculated using Equations (4-4) and (4-5) respectively. Table 4-4 shows these values for Soil Type I, II, and III.

Table 4-4: Damping Coefficients

Soil Type	(H)	V_s	ω_1	ω_2	A	β
-	m	m/s	rad/sec	rad/sec	-	-
I	80	100	1.963	17.671	0.1767	0.00509
II	80	200	3.927	35.343	0.3534	0.00255
III	80	400	1.250	11.250	0.7068	0.00127

4.6 Methodology

To perform dynamic analyses, commercial finite element package PLAXIS (Version 8) is used in this study. The main reason for the selection of this program is its capability and reliability to perform construction stage and soil structure interaction analyses. Plain strain analyses are performed using fifteen nodded triangle elements. Soil assumed to be linear elastic overlaying a rock formation located 80 m below the grade level. Tunnel liner is composed of five nodded Plate (beam) elements. Standard earthquake boundaries used to prevent seismic waves from reflecting back into the soil. The time history is imposed using prescribed displacement boundary condition at the bottom of the model (soil and rock interface). To reduce the effect of the absorbent boundaries they should be place far from the tunnel geometry. Based on some research done by author, it is common practice to make the half-space model at least eight times the thickness of the overburden soil. Therefore, all tunnels are modeled in a 1000 m wide field.

After defining the geometry and boundary conditions, free-field response is created by running the soil model for each case, without presence of the tunnel. Free-field deformations are measured at the end of this stage. Next, the tunnel liner is added to the model, and initial stresses in the soil are created. After creating the initial stresses, first construction stage is used to create (construct) tunnel liner in the soil body. Dynamic analysis is defined and performed as the next stage of the calculation. Here, at the beginning of this stage, all the calculated deformations, and displacements from the previous stage is reset to zero. This is done to make sure that all measured displacements at the end of the dynamic step are only due to the seismic event and no residual displacement will be carried over to this stage from previous stage. Dynamic loads are applied as a prescribed displacement at the bottom of the model, which is assumed as the rock and soil interface. Figure 4-7, 4-8, and 4-9 depict typical mesh used in this study.

(a)

(b)

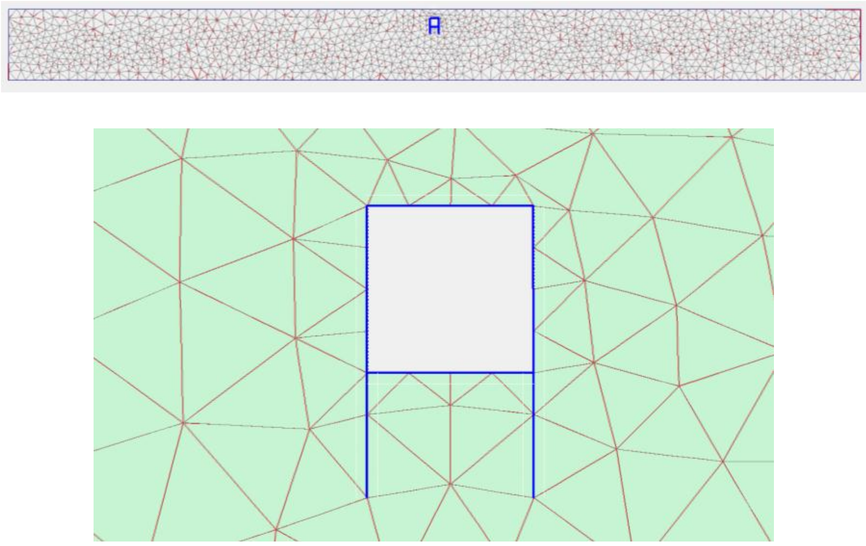

Figure 4-7: Finite element mesh used for Case A; (a) global mesh; (b) enlarged view of the mesh at tunnel location

(a)

(b)

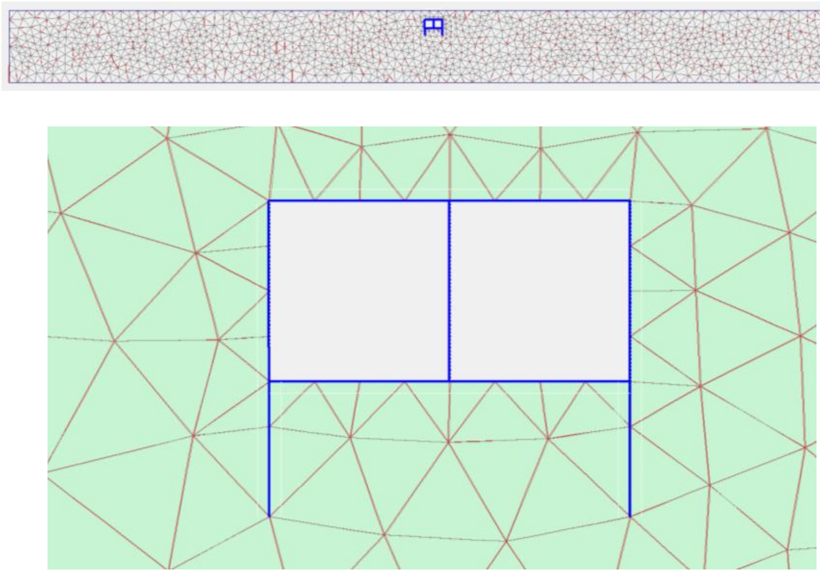

Figure 4-8: Finite element mesh used for Case B; (a) global mesh; (b) enlarged view of the mesh at tunnel location

(a)

(b)

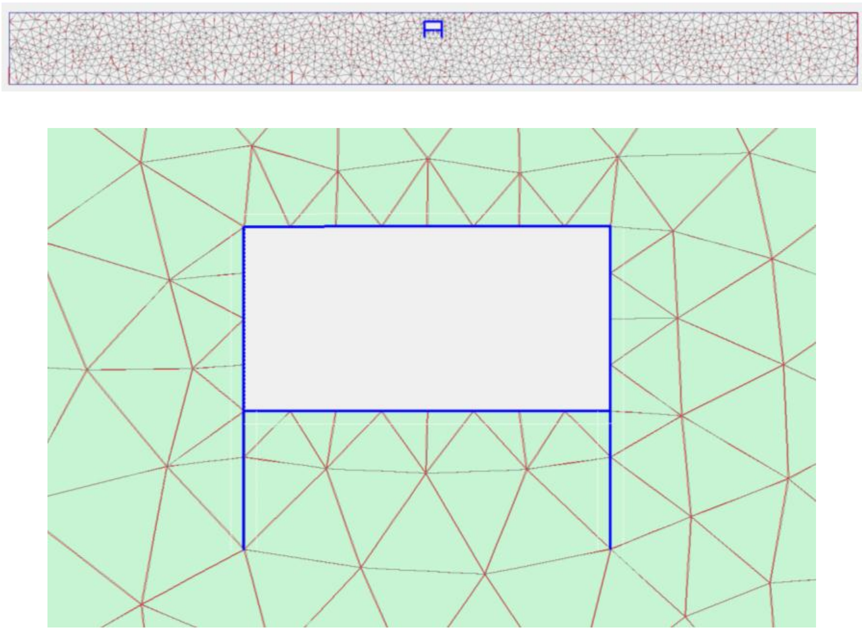

Figure 4-9: Finite element mesh used for Case C; (a) global mesh; (b) enlarged view of the mesh at tunnel location

CHAPTER 5

ANALYSES RESULTS AND DISCUSSION

5.1 Introduction

The results of the finite element analyses are presented in this chapter. After performing dynamic analyses using acceleration time history records mentioned in Table 4-3 for three different soil types, and tunnel geometries A, B, and C, the results for each case are post processed and compared here.

5.2 Tunnel Response Without Initial Support of Excavation

In conventional design, mostly the effect of the initial support of excavation is ignored. Hence, first the finite element results obtained for the Tunnel A without the initial support of excavation (liner only) are presented. The dynamic response (horizontal displacement) of the point A, located on the centerline of the invert, and point B, located on the centerline of the roof, are measured, and subtracted from each other to obtain the maximum relative displacement of these points. These results are then compared with the measured maximum relative free-field displacement of the same two points. Locations of points A and B are shown schematically in Figure 5-1.

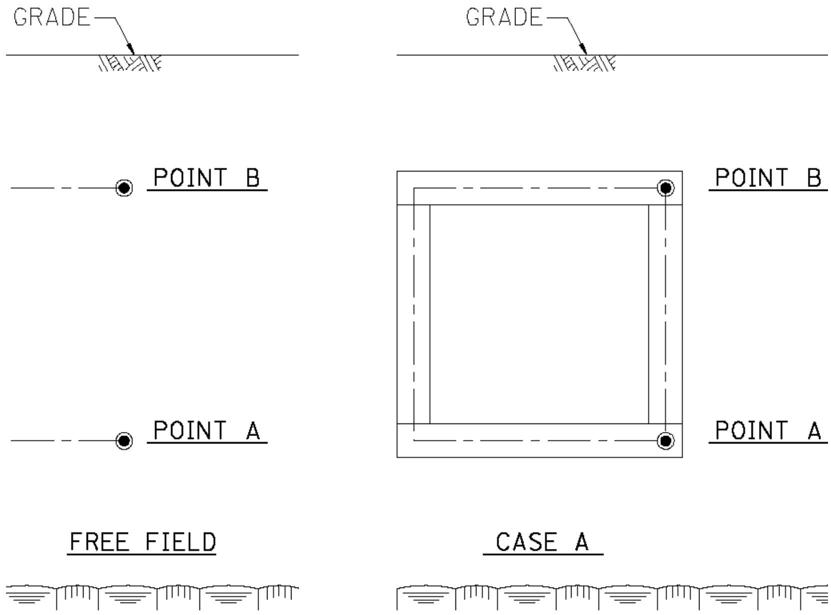

Figure 5-1: Displacement monitoring points

Figure 5-2 compares the relative displacement between points A and B in the free-field with the relative displacement of the same points on the tunnel liner, for Tunnel A, under Duzce ground motion, for Soil type I, II, and III. For the remaining cases the comparison of the maximum free-field relative displacements with the maximum relative displacements of the liner's roof and invert calculated from outputs of the finite element analyses, are presented in Table 5-1. The corresponding estimated deformations obtained using simplified ground-tunnel interaction (Wang, 1993) method is also listed in this table for comparison proposes.

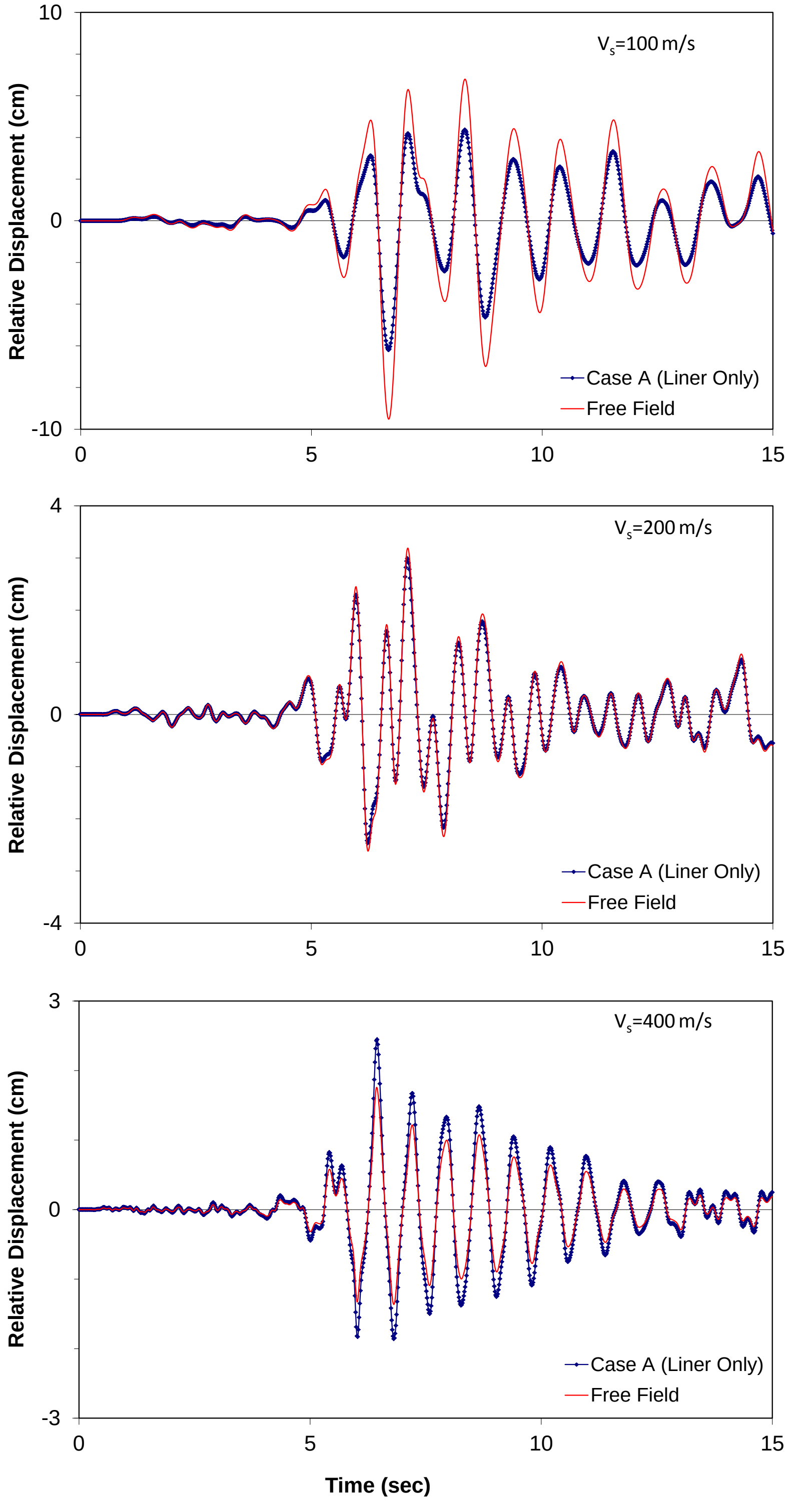

Figure 5-2: Time history response of Case A (Liner only) for Duzce time history for soil type I, II, and III respectively

Inspection of Figure 5-2 shows that for the soil type I (soft soil) with V_s=100 m/s the tunnel response is de-amplified with respect to the free-field response. Furthermore, Table 5-1 indicates that in some cases the ratio of the response reduction could be as high as 40%. Hence, one could conclude that for soft soils, ignoring the tunnel and soil interaction, i.e. using free field deformation method, would result in a conservative design.

On the other hand, from Figure 5-2 and Table 5-1 it is evident that the response of the tunnels in soil type III, (stiff soil) with V_s=400 m/s, is completely different from previous (soft soil) cases. For this soil type, the relative displacement of the tunnel's roof and invert is amplified with respect to free-field relative displacements of the same points (points A and B). In fact, in some cases the calculated displacements for this soil type become more than two times larger than free-field displacements. Hence, it is obvious that for the stiff soil ignoring the tunnel and soil interaction would results in an unrealistic and unsafe design.

Although the results shown for soil type II (medium soil) with V_s=200 m/s in Figure 5-2 are almost similar to soil type I (de-amplification of the response) for Case A, results in the Table 5-1 indicates that this is not the trend for all cases. Actually, for both Case B and C the calculated relative displacements from the finite element analyses are larger than the free-field deformations. Therefore, both increase and decrease in the demand are observed for Soil type II.

Table 5-1 also summarizes the deformation demands obtained from finite element analyses for Case A, B, and C (liner only) with the ones estimated using Wang's (1993) simplified tunnel-ground interaction method. The demands for simplified tunnel-ground interaction method are calculated as follows: first the flexibility ratio and racking coefficient are calculated using Equations 3-1, and 3-2 respectively; then the analytical racking coefficient is multiplied with the free-field deformation obtained from finite element analysis. In Table 5-1, measured maximum relative displacement of the tunnel roof and invert from finite element analyses, are listed next to the values calculated from simplified tunnel-ground interaction for comparison. In Table 5-1, Δ *Wang* represents the calculated demands from simplified tunnel-ground interaction method and Δ *FE* represents the calculated relative displacements from dynamic analyses.

Figure 5-3 compares the tunnel demand obtained using finite element analyses with values obtained using Wang's (1993) simplified tunnel-ground interaction procedure for all motions and tunnels without initial support of the excavation (liner only). Inspection of the Figure 5-3 indicates that the maximum relative displacements obtained from finite element analyses (liner only cases) are in good agreement with the ones estimated using Wang's simplified tunnel-ground interaction procedure.

Table 5-1: Tunnel deformations using Wang Monograph vs. FE Models

MOTION	Geometry	Vs (m/s)	∆ Free Field (cm)	Flexibility Ratio	Racking Coefficient	∆ Wang (cm)	∆ FE (cm)
Duzce	A	100	9.52	0.43	0.58	5.02	6.20
	B	100	9.52	0.53	0.68	5.89	5.45
	C	100	9.52	1.25	1.12	9.69	8.06
	A	200	3.19	1.71	1.36	3.94	2.99
	B	200	3.19	2.21	1.51	4.37	3.69
	C	200	3.19	5.00	2.06	5.97	4.99
	A	400	1.76	6.82	2.22	3.55	2.45
	B	400	1.76	8.47	2.31	3.69	3.28
	C	400	1.76	20.0	2.57	4.10	3.68
Cape Mendocino	A	100	6.01	0.43	0.58	3.17	3.91
	B	100	6.01	0.53	0.68	3.72	3.44
	C	100	6.01	1.25	1.12	6.12	5.09
	A	200	2.30	1.71	1.36	2.84	2.08
	B	200	2.30	2.21	1.51	3.15	2.43
	C	200	2.30	5.00	2.06	4.30	3.15
	A	400	1.72	6.82	2.22	3.47	2.38
	B	400	1.72	8.47	2.31	3.61	3.24
	C	400	1.72	20.0	2.57	4.01	3.65
Loma Prieta	A	100	1.91	0.43	0.58	1.01	1.28
	B	100	1.91	0.53	0.68	1.18	1.14
	C	100	1.91	1.25	1.12	1.95	1.62
	A	200	1.42	1.71	1.36	1.76	1.36
	B	200	1.42	2.21	1.51	1.95	1.65
	C	200	1.42	5.00	2.06	2.66	2.16
	A	400	0.51	6.82	2.22	1.04	0.75
	B	400	0.51	8.47	2.31	1.08	1.08
	C	400	0.51	20.0	2.57	1.20	1.24

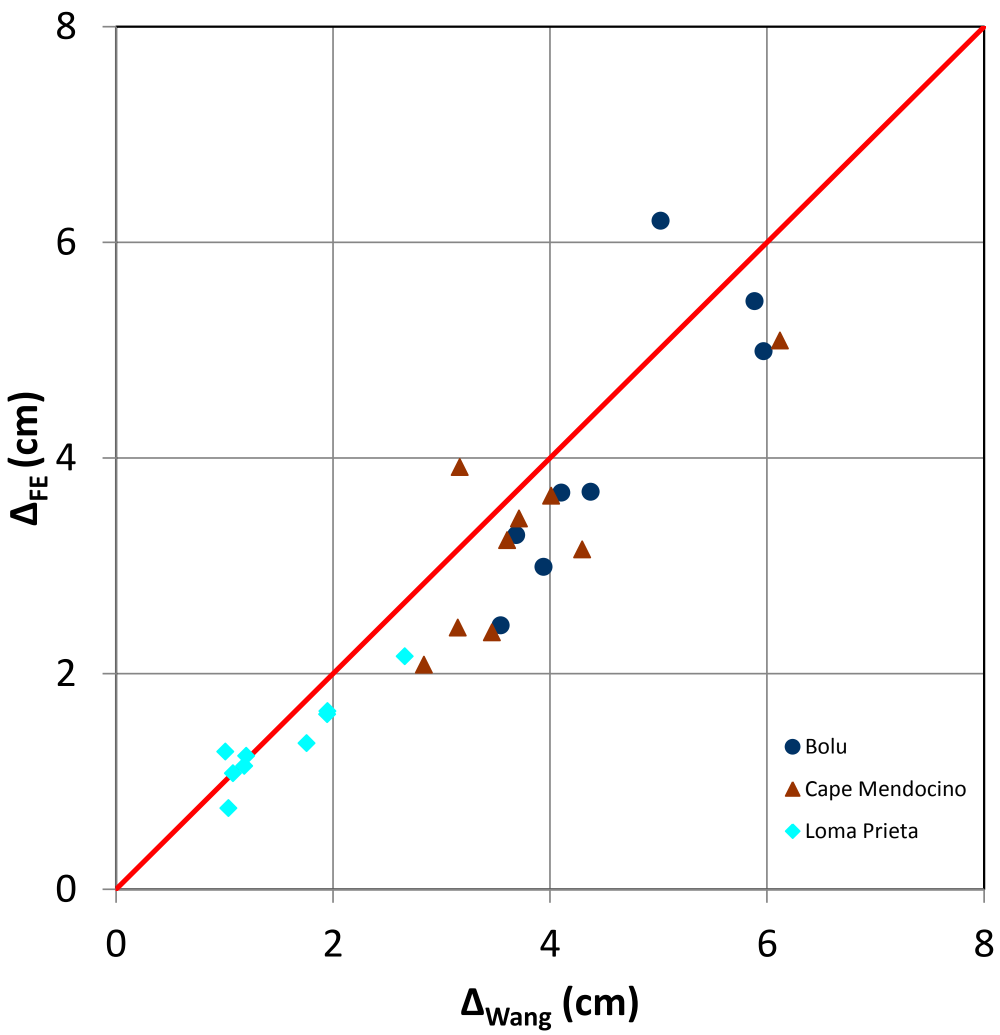

Figure 5-3: Wang Displacement vs. FE Displacements

5.3 Effect of the Initial Support System

To illustrate the effect of the initial support of excavation on the seismic behavior of the cut and cover tunnels, the maximum relative deformation of the tunnel and initial support system, obtained from finite element analyses are normalized with the maximum relative deformations of the liner only case. This procedure is repeated for each embedment depth and the results are shown in Figures 5-4 to 5-6. Here, for calculating the maximum relative displacements, the same points (point A and B, see Figure 5-1) are used as previously shown in Section 5.2. This is done mainly to make sure that the comparisons of the demands have the same reference point. Again, since the initial support systems are mostly ignored in the conventional design, the selection of the same reference points seems the best choice for the comparison proposes.

In Figures 5-4 to 5-6, the first character of the legend is representing the geometry cases, namely Case A, Case B, or Case C, and numbers 1, 2, and 3 are used for Duzce, Cape Mendecino, and Loma Prieta motions respectively. For example B2, represents the demand for Case B under Cape Mendocino motion.

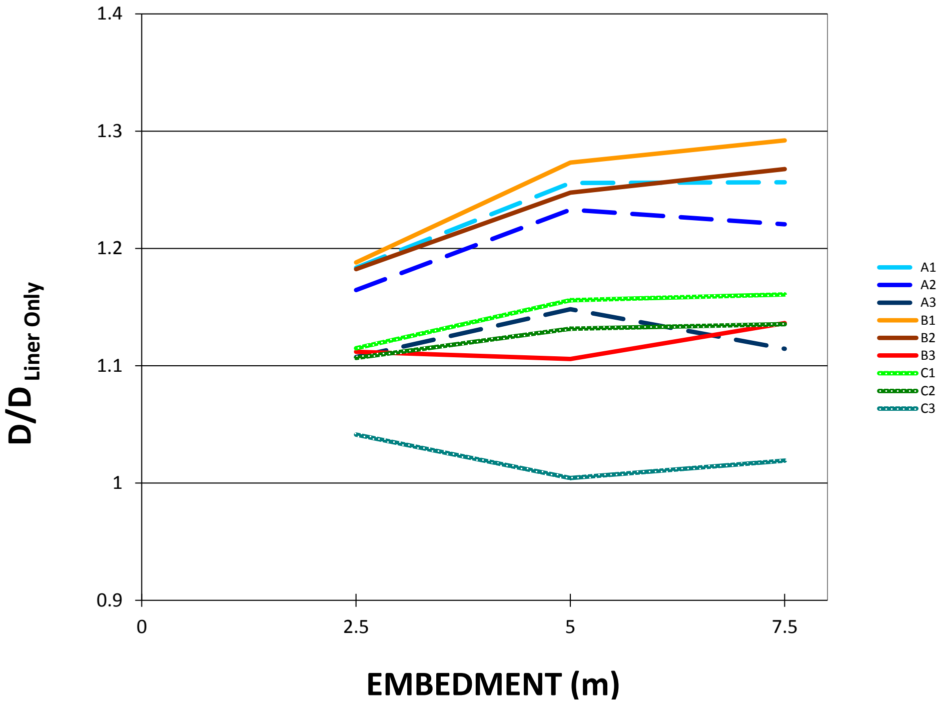

Figure 5-4: Normalized displacement of cut and cover tunnel for soil type I

Figure 5-4 depicts the normalized relative displacements for various embedment depths and for each geometry in soil type I (soft soil) with V_s=100 m/s. For this type of soil, the deformation demands of the tunnels show an increase up to 19%, when the initial support of excavation with 2.5 m embedment length is accounted for in the analyses. As the embedment length of the initial support increases from 2.5 m to 5.0 m, the amplifying trend continues except for Case B3 and Case C3. However, when the embedment length is increased to 7.5 m the rate of the demand increase is not as significant as it was before. Furthermore, when the embedment is increased to 7.5 m for certain cases the demand decreases compared to 5.0 m embedment. Interestingly the demand decreases for

Cases B3 and C3 when the embedment increased to 5.0 m and increases again when the embedment becomes 7.5 m.

Due to the mix responses for different geometries, one can conclude that the overall demand of the tunnels, are affected by the embedment length of the initial support of the excavation and the ground motion parameters. For different ground motions, the interactions between soil and tunnels are not the same.

For soil type II (medium soil) with V_s=200 m/s, the normalized maximum relative displacements depicted in Figure 5-5 indicate that the initial support of the excavation changes the dynamic demand of the tunnels. However, this change does not seem to be as significant as it was for soft soil. Nevertheless, the change in the demands when the initial support of the excavation is accounted for in the analyses can be as high as 12%. Interestingly the results for 2.5 m, 5.0 m, and 7.5m embedment lengths are very similar, and the embedment length variation does not seem to be as important as it was in the soft soil.

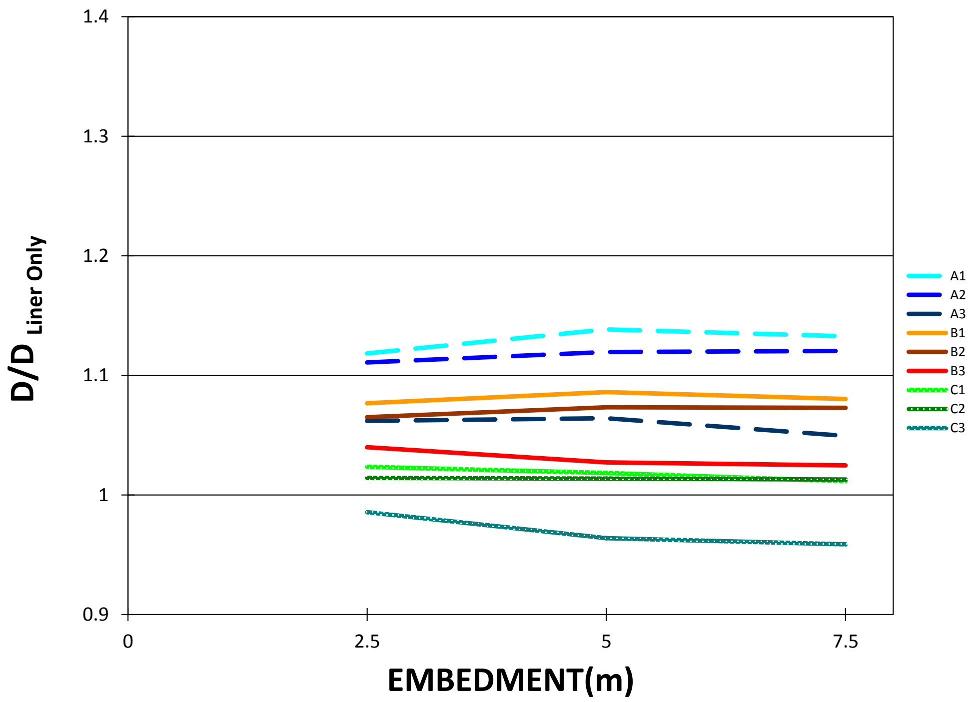

Figure 5-5: Normalized displacement of cut and cover tunnel for soil type II

The normalized maximum relative displacements of the three cases, namely Case A, Case B, and Case C, for soil type III (stiff soil) with V_s=400 m/s, are presented in Figure 5-6. Inspection of the results presented in this Figure, indicates that, once again, the embedment depth of the initial support of the excavation, has minimal effect on the overall demand of the tunnels for the soil type III (stiff soil). For stiff soil case, the deformation trends are very similar for each geometry type, and all three motions. Case A shows some amplified demand for all embedment depths, for Case B the existence of the initial support of the excavation does not seem to affect the dynamic demand of the tunnel and for Case C the initial support of the excavation reduces the dynamic demands.

Therefore, it can be concluded that the response of the tunnel is more sensitive and dependent to the tunnel liner properties than the ground motion parameters for Soil type III.

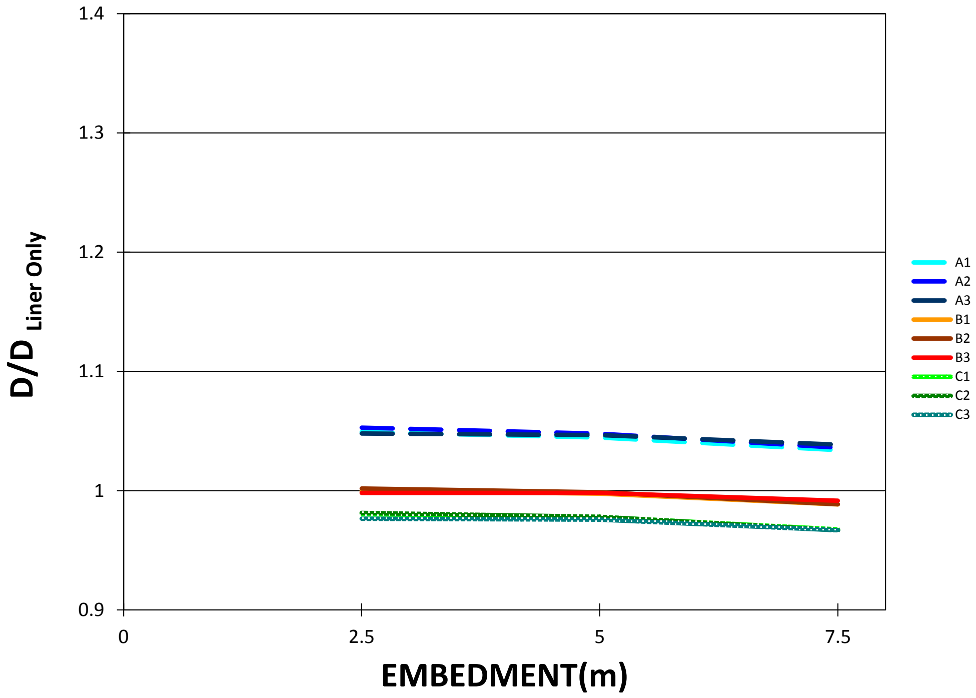

Figure 5-6: Normalized displacement of cut and cover tunnel for soil type III

5.4 Comparison of the Dynamic Demands with Free-Field Deformations

Since free field racking method is also widely used in practice, which ignores soil-tunnel interaction, the obtained results with and without initial support of the excavation are normalized with free-field deformations and presented next. As it was explained in section 5.2, for the comparison purposes, the maximum relative displacements are monitored at points A and B shown in Figure 5-1 .The results are presented in Figures 5-7 to 5-9.

Figure 5-7 depicts the normalized maximum tunnel relative displacements (liner only as well as liner with initial support of the excavation) with maximum measured free-field displacements for soil type I (soft soil) with V_s=100 m/s.

It clearly shows an increase in the demand for all cases as the initial support of the excavation (2.5 m embedment length) is added to the system. The effect of the additional length clearly decreases as the embedment length of the initial support of the excavation increases from 2.5 m to 5.0 m. There are minor changes in the response, when the embedment length is changed from 5.0 m to 7.5 m.

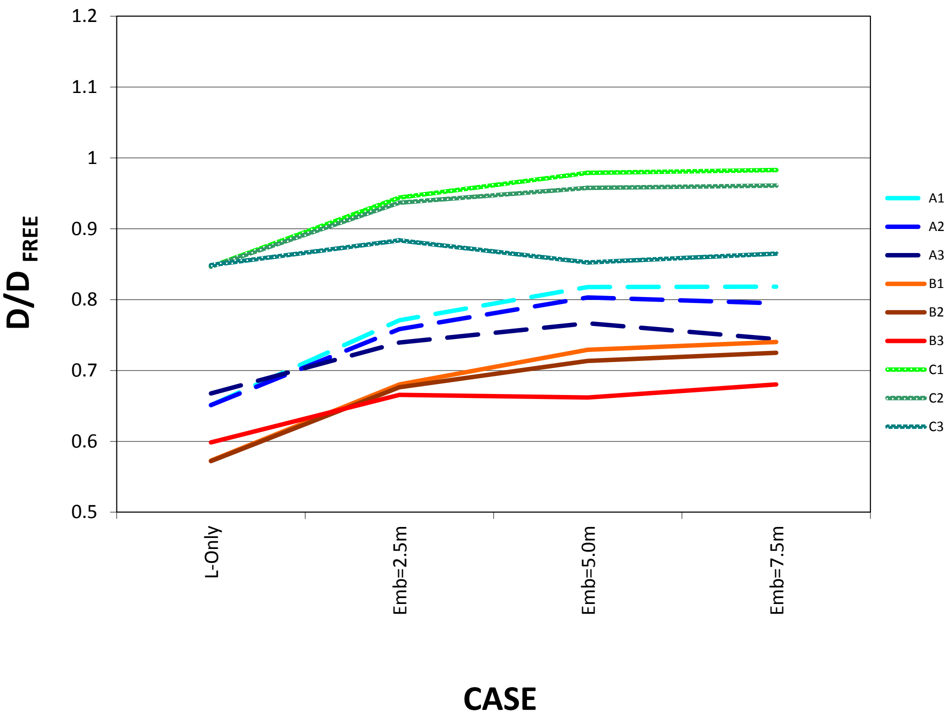

Figure 5-7: Normalized displacement of cut and cover tunnel for soil type I

The same procedure is repeated for soil type II (medium soil) with V_s=200 m/s, and the results are shown in Figure 5-8. Here, the effect of the initial support of the excavation on the maximum relative displacement response of the tunnels for the first 2.5 m embedment length can be seen clearly. As the embedment, length is increased from 2.5 m to 5.0 m and then 7.5 m there are minor variations in the normalized maximum relative displacements between the tunnels' roof and invert.

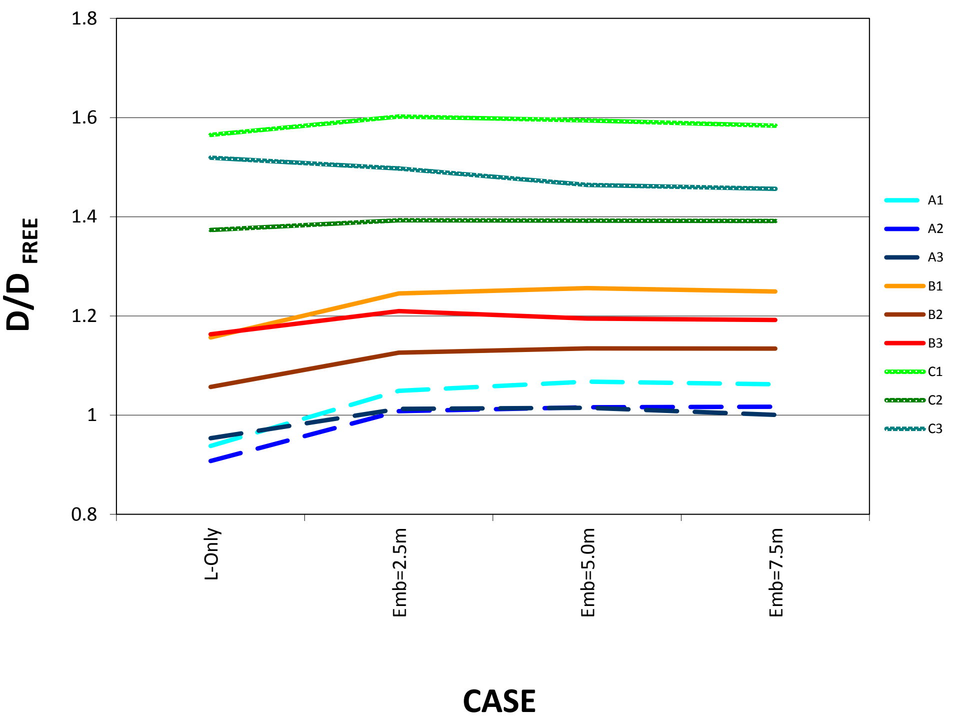

Figure 5-8: Normalized displacement of cut and cover tunnel for soil type II

Figure 5-9 depicts the normalized results for Case A, B, and C obtained for three different acceleration time histories for type III (stiff soil) with V_s=400 m/s.

As previously mentioned in Section 5.2, for stiff soil the soil-tunnel interaction becomes dominant. The results are significantly amplified. However, there is no significant change in the demand due to the initial support of the excavation and its embedment depth. The overall amplified demands, with respect to the free-field maximum relative displacements, show some minor increase or decrease, depending on the geometry.

For Case A, adding the first 2.5 m embedded initial support of the excavation to the system increases the already amplified demand slightly. Additional embedment length has minor effect on the dynamic demand of the tunnels. For Case B, the demand remains almost unchanged for liner only case and all other different embedment depths of the initial support of excavation. Case C shows a different response. As the initial support of the excavation is added to the system, there is a minor decrease in the calculated maximum relative displacement. For the next two cases, i.e. 5.0 m, and 7.5 m embedment lengths, there is no change in the calculated maximum relative displacements for Case C. It is important to mention that all these analyses and their results are based on assumption that, the medium that the tunnel structure is built in is soil. The results mentioned above shall not be used for tunnel structures in solid rock.

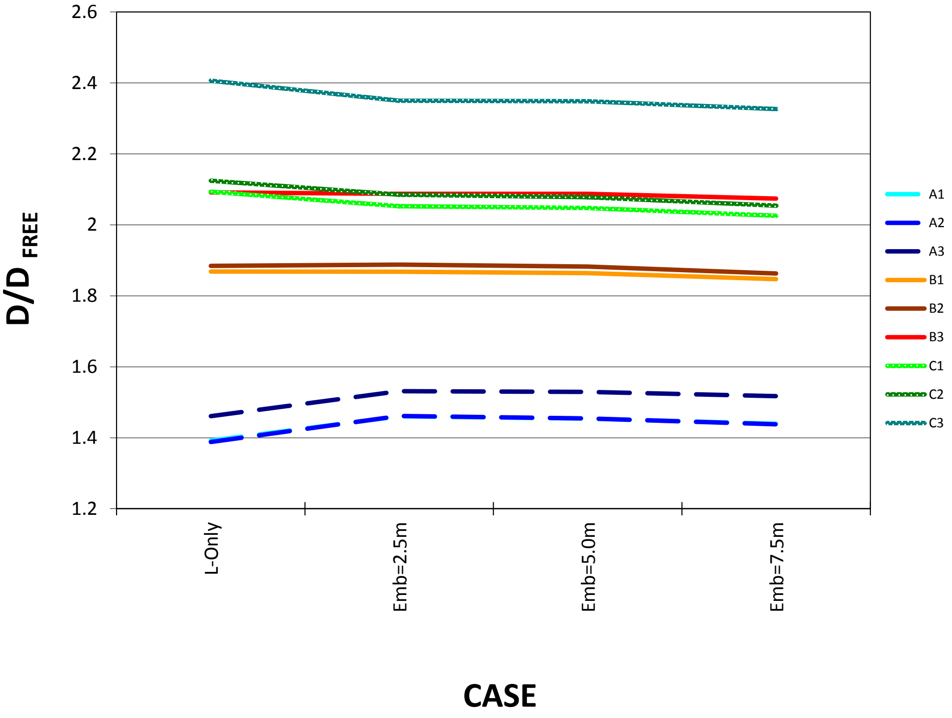

Figure 5-9: Normalized displacement of cut and cover tunnel for soil type III

CHAPTER 6

CONCLUSIONS AND RECOMMENDATIONS

6.1 Conclusions

The main objective of this study is to investigate the effect of the initial support of the excavation with variable embedment depth on the seismic behavior of the cut and cover structures. Dynamic analyses on three different geometries and soil properties were performed using commercial finite element program PLAXIS (Version 8). Three different time histories were used to capture possible motion dependent behaviors.

Racking of cut and cover structures is one of the most important and dominant deformation mode that need to be accounted in the seismic design. Due to the existence of soil-structure interaction, the task of predicting the racking demand of the tunnel requires rigorous analyses, such as dynamic analyses. Dynamic analyses for underground structures are complicated and very time consuming in nature. Therefore, as it was mentioned in Chapter 3 simplified methods have been developed to help engineers to predict and include these types of forces in their design. The best-known approaches are the free-field deformation method and simplified tunnel-ground interaction method proposed by Wang (1993).

Construction of cut and cover structure in soil usually requires installation of the initial support of excavation system, which mostly are rigid type of initial supports, such as tangent piles or secant piles. These systems usually remain in place after completion of the final structure. However, it is a common practice to ignore the contribution of initial support for the design. Furthermore, in simplified seismic analyses method, it is not possible to include and account for the effect of the initial support of the excavation.

In this study, the effects of initial support of excavation on the seismic performance of cut and cover tunnels is investigated by means of a detailed dynamic finite element analysis. Results of the study show that depending on the soil stiffness (soft, medium, or stiff soil), the dynamic response of the tunnel deformations are affected by the initial support of excavation.

- For soft soils with V_s=100 m/s, ignoring the tunnel-soil interaction, i.e. using free-field deformation method results in conservative design. That is, for soft soils free-field deformation method is not recommended to estimate seismic demand.

- For stiff soils with V_s=400 m/s, ignoring the tunnel-soil interaction by using the free-field deformation method, results in an unrealistic, and unsafe design. Again, for stiff soils the free-field deformation method is not recommended.

- When the effect of initial support of the excavation is ignored, the seismic demands obtained by using dynamic finite element analyses match closely with the ones estimated using simplified tunnel-ground interaction method by Wang (1993).

- For soft soil, the tunnel deformation demands generally increase when the initial support of the excavation is accounted for in the analyses. Significant amplifications (up to 29%) are observed when the initial support system with varying embedment length is added to the finite element models. It is also observed that overall response is affected by the details of the ground acceleration in addition to initial supports' embedment.

- As the soil characteristics improves the effect of the initial support of excavation and its embedment diminishes. Nevertheless, for medium soils (V_s=200 m/s) and for stiff soils (V_s=400 m/s), the existence of the initial support of excavation amplifies the demands 14% and 5% respectively. For some cases reductions up to 5% is observed as well. For all investigated cases, the drift ratio between the top and bottom of the structures is less than 1%. This indicates that for all cases the structures remain in the elastic range.

6.2 Recommendations for Future Research

Results presented in this study are only valid for the tunnel geometries/ configurations given in Chapter 4 and assumptions made for this study. Given the complexity of the problem, further parametric analysis should be conducted for different tunnel geometries, different overburden, different bedrock depth, and additional ground motion time histories.

REFERENCES

ASCE, Earthquake damage evaluation and design considerations for underground structures, February. American Society of Civil Engineers, Los Angeles Section, 1974.

AASHTO, American Association of State Highway and Transportation Officials, Standard Specifications of Highway Bridges, 17th Edition., Washington D.C., 2002.

F. Ostadan and W. H. White, "Lateral Seismic Soil Pressure - An Updated Approach", Bechtel Technical Grant report, 1997.

Hashash, Y.M.A., Hook, J.J., Schmidt, B., Yao, J.I., Seismic design and analysis of underground structures, Tunneling and Underground Space Technology 16, pp. 247–293, 2001.

Kaneshiro, J.Y., Power, M., Rosidi, D., 2000. Empirical correlations of tunnel performance during earthquakes and aseismic aspects of tunnel design. Proceedings of the Conference on Lessons Learned From Recent Earthquakes - On Earthquakes in Turkey 1999, November 8-11.

Kuesel, T.R., Earthquake Design Criteria for Subways, J. Struct. Div., ASCE ST6, pp. 1213-1231, 1969.

Mononobe, N., Matsuo, H., On The Determination of Earth Pressures During Earthquakes, Proceedings of World Engineering Congress, 1929.

Owen, G.N., Scholl, R.E. Earthquake engineering of large underground structures. Report no. FHWA-RD-80-195. Federal Highway Administration and National Science Foundation, 1981.

Penzien, J., Seismically induced raking of tunnel linings, Earthquake Engineering and Structure Dynamics 29, pp. 683–691, 2000.

Okabe, S., General theory on earth pressure and seismic stability of retaining wall and dam, Journal of Japan Society of Civil Engineers, Vol. 12, No. 1, pp. 123-134, 1926.

Power, M., Rosidi, D., Kaneshiro, J. Seismic vulnerability of tunnels revisited. In: Ozedimir, L., (Ed.). Proceedings of the North American Tunneling Conference. Elsevier, Long Beach, CA, USA, 1998.

Merritt, J.L., Monsees, J.E., Hendron, A.J., Jr., Seismic design of underground structures, Proceedings of the 1985 Rapid Excavation Tunneling Conference, vol. 1, pp. 104-131, 1985.

Stevens, P.R. A review of the effects of earthquakes on underground mines. United States Geological Survey Open File Report 77-313. US Energy Research and Development Administration, Reston, VA, 1997.

Dowding, C.H., Rozen, A. Damage to rock tunnels from earthquake shaking. J. Geotech. Eng. Div., ASCE 104 (GT2), pp.175-191, 1978.

Technical Manual for Design and Construction of Road Tunnels – Civil Elements. U.S. Department of Transportation, Federal Highway Administration, Publication No. FHWA- NH1-10-034, 2009.

Wang, J. M., “The Distribution of Earthquake Damage to Underground Facilities during the 1976 Tangshan Earthquake,” Earthquake Spectra, Vol. 1, No. 4, 1985.

Wang, J.-N. Seismic Design of Tunnels: A State-of-the-Art Approach, Monograph, monograph 7. Parsons, Brinckerhoff, Quade and Douglas Inc, New York, 1993.

Wood, J. H., “Earthquake-Induced Soil Pressures on Structures,” Report No. EERL 73-05, California Institute of Technology,1973.

http://nisee.berkeley.edu., Website of National Information Service for Earthquake Engineering. PEER, NGA Strong Motion Database.

APPENDICES

Table A-1: Tunnel deformation demands calculated from FE Models

MOTION	Vs (m/s)	Δ Free-Field (cm)	Geometry	Δ FE Liner Only (cm)	Δ FE L = 2.5 m (cm)	Δ FE L = 5.0 m (cm)	Δ FE L = 7.5 m (cm)
Duzce	100	9.52	A	6.200	7.338	7.786	7.760
			B	5.453	6.478	6.943	7.046
			C	8.062	8.988	9.319	9.359
	200	3.19	A	2.989	3.343	3.403	3.386
			B	3.686	3.969	4.003	3.982
			C	4.989	5.107	5.081	5.047
	400	1.76	A	2.446	2.566	2.555	2.529
			B	3.283	3.282	3.275	3.245
			C	3.679	3.607	3.598	3.560
Cape Mendocino	100	6.01	A	3.914	4.558	4.826	4.777
			B	3.438	4.065	4.289	4.358
			C	5.088	5.631	5.757	5.777
	200	2.30	A	2.083	2.314	2.332	2.334
			B	2.426	2.584	2.604	2.603
			C	3.152	3.197	3.195	3.193
	400	1.72	A	2.383	2.509	2.497	2.469
			B	3.236	3.242	3.232	3.199
			C	3.648	3.580	3.568	3.527
Loma Prieta	100	1.91	A	1.276	1.413	1.465	1.422
			B	1.144	1.272	1.265	1.300
			C	1.622	1.689	1.629	1.653
	200	1.42	A	1.355	1.439	1.442	1.422
			B	1.653	1.719	1.698	1.694
			C	2.159	2.128	2.081	2.070
	400	0.51	A	0.751	0.787	0.786	0.780
			B	1.075	1.073	1.073	1.066
			C	1.273	1.208	1.207	1.196

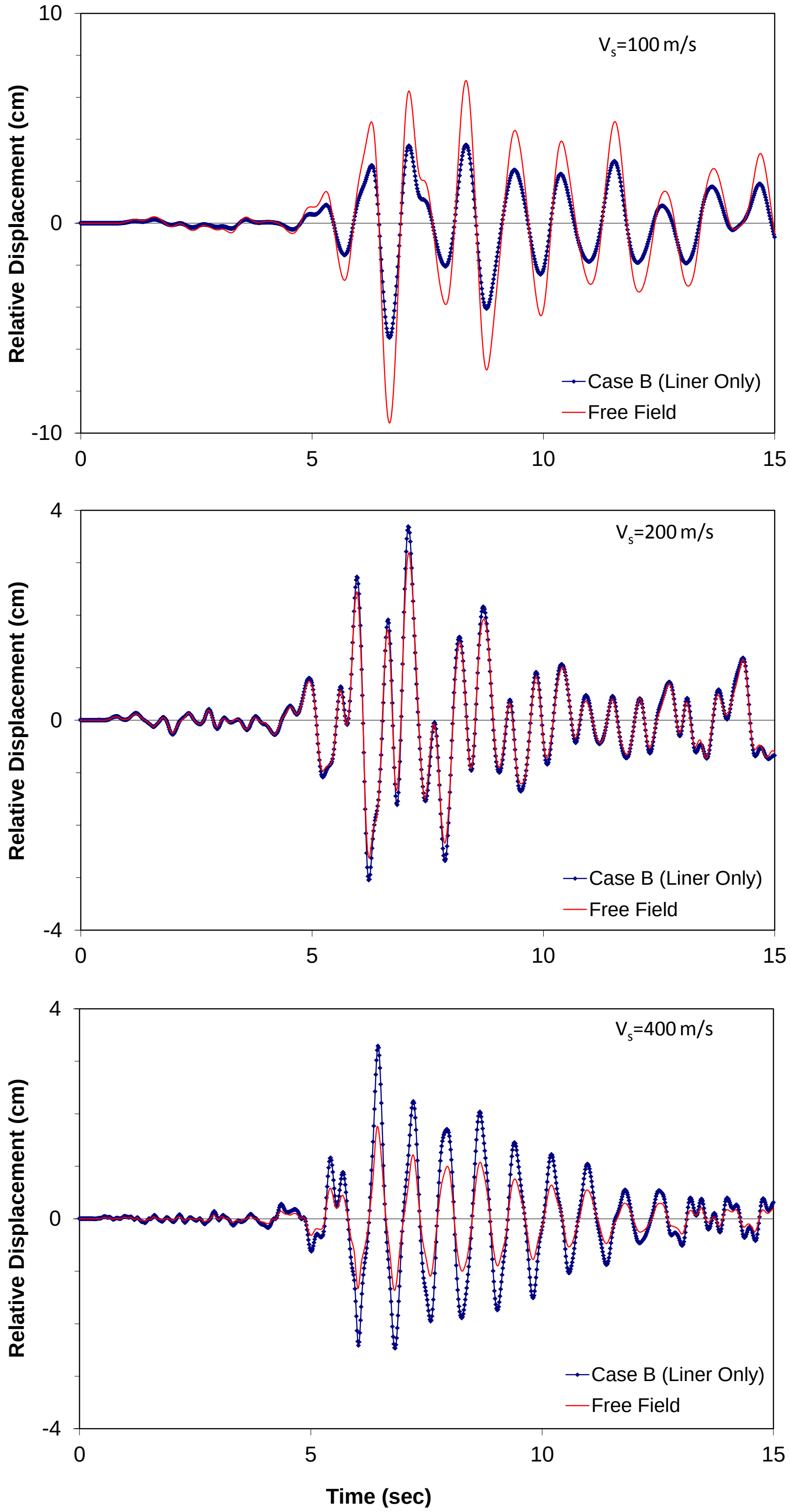

Figure A-1: Time history response of Case B (Liner only) for Duzce time history for soil type I, II, and III respectively

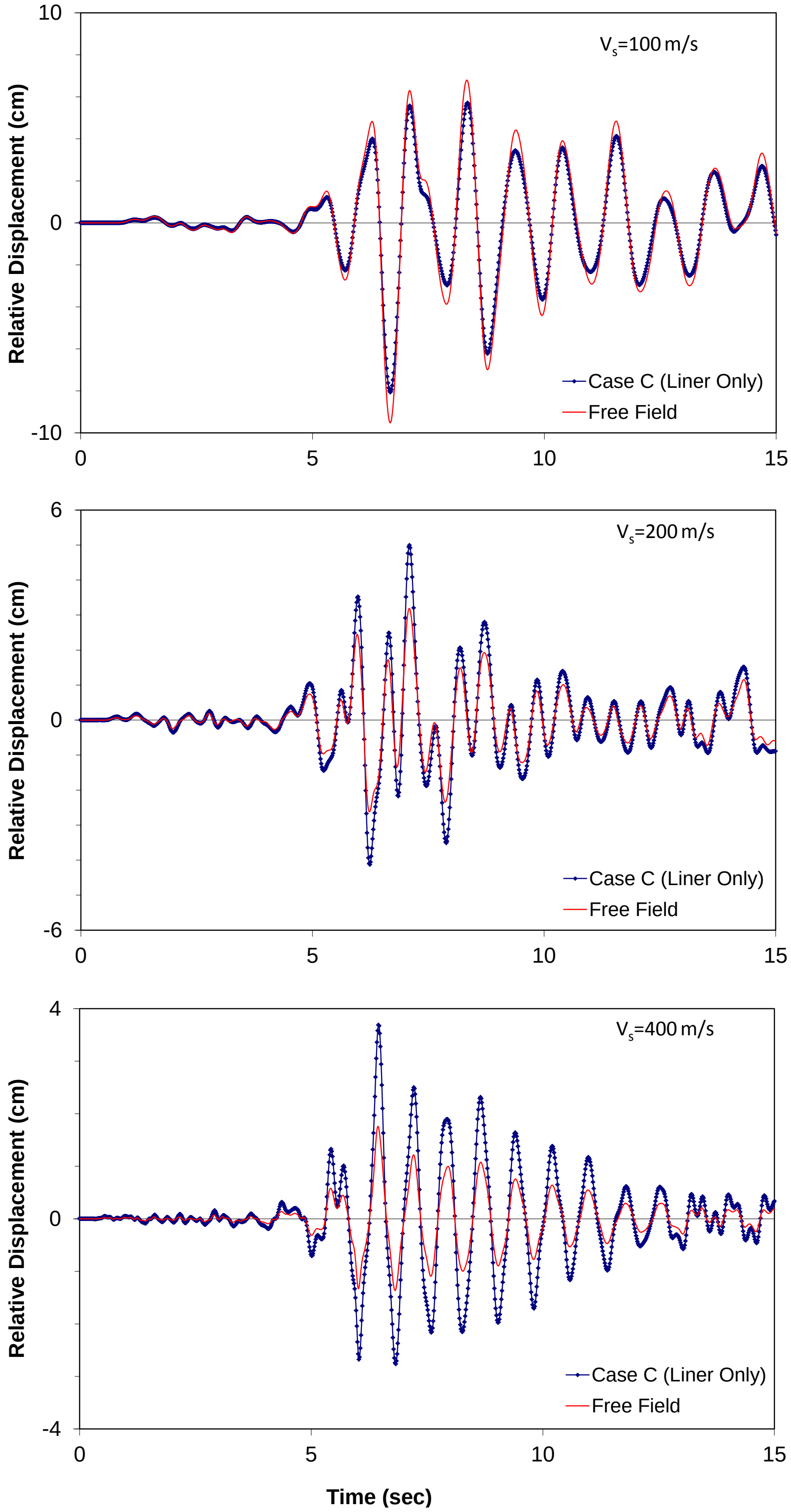

Figure A-2: Time history response of Case C (Liner only) for Duzce time history for soil type I, II, and III respectively